To appear in AJ
Preprint typeset using LaTeX style emulateapj v. 08/13/06

arXiv:0909.3936v1 [astro-ph.GA] 22 Sep 2009

MASS DISTRIBUTION IN HICKSON COMPACT GROUPS OF GALAXIES

H. Plana [1,2], P. Amram [2], C. Mendes de Oliveira [3], C. Balkowski [4]

To appear in AJ

ABSTRACT

This study presents the mass distribution for a sample of 18 late-type galaxies in nine Hickson Compact Groups. We used rotation curves from high resolution 2D velocity fields of Fabry-Perot observations and J-band photometry from the 2MASS survey, in order to determine the dark halo and the visible matter distributions. The study compares two halo density profile, an isothermal core-like distribution and a cuspy one. We also compare their visible and dark matter distributions with those of galaxies belonging to cluster and field galaxies coming from two samples: 40 cluster galaxies of Barnes et al. (2004) and 35 field galaxies of Spano et al. (2008).

The central halo surface density is found to be constant with respect to the total absolute magnitude similar to what is found for the isolated galaxies. This suggests that the halo density is independent to galaxy type and environment. We have found that core-like density profiles fit better the rotation curves than cuspy-like ones. No major differences have been found between field, cluster and compact group galaxies with respect to their dark halo density profiles.

Subject headings: galaxies: halos — galaxies: kinematics and dynamics — galaxies: general

1. INTRODUCTION

Hickson Compact Groups of Galaxies (HCGs) are collections of three to seven galaxies inside a three magnitude interval, where the members have a projected separation of the order of the galaxy diameters and a low velocity dispersion ($\sim$200 km.s^{-1}, Hickson 1992). These galaxies, located in the denser environments of the local universe, experience a high rate of galaxy-galaxy interactions and merging. They constitute a privileged laboratory to study different stages of interactions from violent merging to systems with no apparent signs of interaction.

Rubin et al. (1991) analyzed rotation curves for 32 Hickson compact group galaxies and found that two-thirds of them had peculiar rotation curves. For the sub-sample of galaxies for which rotation curves could be derived, they found that spiral galaxies in compact groups have low mass-to-light ratios compared to field galaxies by about 30%, which could be explained if compact group galaxies have smaller dark halos than their field counterparts. Given that compact groups are environments where tidal encounters are common, it may be expected that interactions have stripped or disrupted the galaxy dark halos at some level. These conclusions have important consequences for the determination of group lifetimes and understanding how compact groups evolve and eventually merge.

In order to address these questions, we have launched an observational program to obtain and analyze 2D velocity fields of HCGs using scanning Fabry-Perot techniques. Fabry-Perot imaging of about 30 groups (about 100 galaxies) have be obtained to date. Specific groups have been studied such as HCG 16 (Mendes de Oliveira et al. 1998), HCG 92 (Plana et al. 1999; Mendes de Oliveira et al. 2001), HCG 31(Amram et al. 2004, 2007), HCG 90 (Plana et al. 1998), HCG 18 (Plana et al. 2000) and HCG 79 (Durbala et al. 2008). HCG 07, HCG 10, HCG 19, HCG 87, HCG 91 and HCG 96 have been studied by Amram et al. (2003) and Plana et al. (2003) studied HCG 88, HCG 89, HCG 100. Torres et al. (2009) studied the kinematics and the star formation in the intragroup medium in HCG 02, HCG 22 and HCG 23. A determination of a group evolutionary sequence was done by Plana et al. (2002) and the study of the Tully-Fisher (T-F) relation of the galaxies in these dense environments was done by Mendes de Oliveira et al. (2003). They have shown, for a sample of 25 rotation curves of late-type galaxies, that HCG galaxies follow the (T-F) relation but a few galaxies are brighter than expected from the relation with their mass or, alternatively, present a mass that is too low for their luminosities. Mendes de Oliveira et al. (2003) favor a scenario in which these outliers have been brightened because of either enhanced star formation or merging. Alternatively, the CG galaxies may have undergone truncation of their dark halo due to interactions. The fact that the B-band T-F relation is similar for compact group and field galaxies tells us that these galaxies show common mass-to-size relations and that the halos of compact group galaxies have not been significantly stripped inside R$_{25}$.

In this paper, we address the question of the mass distribution (luminous and dark) of spiral galaxies in compact groups in order to determine whether galaxies in dense environments have experienced a different history than galaxies in less dense environments. This work extends the study by Mendes de Oliveira et al. (2003) on the dynamics of galaxies in compact groups by investigating the distribution of the mass, taking into account the contribution of the bulge, the disk and the dark halo. To quantity the mass distribution of galaxies we have used

---

[1] Laboratorio de Astrofísica Teórica e Observacional, Universidade Estadual de Santa Cruz, Rodovia Ilhéus - Itabuna km 16 45650-000 Ilhéus BA - Brazil

[2] Laboratoire d'Astrophysique de Marseille, Université de Provence, CNRS, 38, rue Frédéric Joliot-Curie 13388 Marseille cedex 13 France

[3] Universidade de São Paulo Instituto de Astronomia, Geofísica e Ciências Atmosféricas, Departamento de Astronomia, Rua do Matão 1226 - Cidade Universitária 05508-900 São Paulo SP - Brazil

[4] Observatoire de Paris, GEPI Université Paris 7, CNRS, 5 Place Jules Janssen, F-92195 Meudon Cedex, France

mass models based on Hα rotation curves and surface brightness profiles. We could not derive extended rotation curves, with combined Hα and HI data, as done by Spano et al. (2008) (hereafter S08) for galaxies in looser environments, given that there are no HI rotation curves available for the compact group galaxies in our sample. Different profiles have been tested to model dark halos. The mass-to-light fraction of the disk is computed together with the dark halo parameters using the best fit model (hereafter BFM) and the maximum disk model (hereafter MDM). The MDM approach uses the exponential disk in order to fit the rotation curve. With the MDM approch we use the ISO hypothesis to model the halo.

The paper is structured as follows. In section 2, we present the data and models (photometric and kinematic). In section 3, we review the mass distribution of galaxies in the field and in clusters. In section 4 we present, analyze and discuss our results on HCGs and compare them to results in less dense environments. Finally in section 5, some concluding remarks are given. In appendix (A) we describe individually the RCs for each galaxy and in appendix (B), from figure 4 to figure 21, we present the J-band surface brightness profile and the RCs for the galaxies studies.

2. DATA AND MODELS

We have used the 2MASS survey (Skrutskie et al. 2006) to compute the photometric surface brightness profiles. Images from the 2MASS survey are already calibrated with a given zero point for each field and with a pixel size of $1''$ on the sky. This pixel size is well matched to the pixel size of the Fabry-Perot maps of $0.91''$ (Amram et al. 2003; Plana et al. 2003).

We have built surface brightness profiles using the J-band because it probes the dominant stellar component out to the outskirts.

We have selected a sub-sample of 18 galaxies among the 25 galaxies used in the Mendes de Oliveira et al. (2003) study. Indeed, 2MASS data are not exploitable for seven of them: four galaxies (HCG19c, HCG79d, HCG89d, HCG96d) show J-images that are too weak to be exploited and three others (HCG100c, HCG100d, HCG96a) prove to be too difficult to derive satisfactory surface brightness profiles.

Surface brightness profiles have been built by fitting ellipses to the isophotes of the J-band images using the *ELLIPSE task* of the *SDSDAS package* with IRAF [5]. We only fixed the center of the ellipse in the fitting parameters and we usually used a $0.2''$ space between two ellipses. In a few cases (for HCG07c, HCG16c, HCG19a, HCG88d), we had to extrapolate the outer profile using an exponential disk profile in order to reach the same extension as the rotation curves since the sky background contaminates the surface brightness profile.

In order to use the mass model, we have performed a decomposition of the surface brightness profile into classical two components: an exponential disk

$$\mu = \mu_0 + 1.0857\frac{r}{h} \tag{1}$$

where μ_0 is the central surface brightness and h is the disk scale parameter,

and a bulge with an $r^{1/4}$ law

$$\mu = \mu_e + 8.3268\left[(\frac{r}{r_e})^{1/4} + (\frac{r}{r_t})^4\right] \tag{2}$$

where μ_e is the central surface brightness, and r_e and r_t are scale factors.

To perform the decomposition we used a home-made program based on a minimized χ^2 routine from the MINUIT package (Fletcher 1970). The program first fits the disk using a visual estimate of the profile. It then subtracts the fitted disk and adjusts the bulge. The operation is repeated in order to minimize the χ^2 for each disk and bulge parameter. Using this method, the structures seen in the disk surface brightness profiles are carried on to the mass profiles. We then have five parameters, two for the disk (μ_0 and h) and three for the bulge (μ_e, r_e and r_t). Table 1 shows the results of the fit. We also list the values of inclination used to derive the rotation curves, from velocity fields, published in Amram et al. (2003), Plana et al. (2003) and Mendes de Oliveira et al. (1998).

In order to compute the mass distribution, we have combined the stellar light contribution derived from the photometry with the dark halo contribution from the rotation curves using the model developed by Carignan & Freeman (1985) and revised by Blais-Ouellette et al. (2001). The surface brightness profile is transformed into a mass distribution for the stellar disk and the stellar bulge assuming a variable but radially constant mass-to-light ratio M/L (Casernato 1983; Carignan & Freeman 1985). Mass decompositions into luminous and dark components are not unique, mainly due to the uncertainties of the stellar disk M/L (Barnes et al. 2004) but also due to our ignorance of the actual dark halo density profile. We minimized this problem by using J-band photometry in order to narrow down the stellar component to the old stellar populations. This mass model estimates the contribution of each velocity component (bulge, disk and halo) using the photometric profile decomposition for the luminous contribution (bulge and disk) and a predetermined density profile for the halo.

The luminosity profile, in the J-band, is used to probe the mass-dominant stellar component and this is transformed into a mass distribution for the stellar disk assuming a variable but radially constant M/L ratio for the disk and the bulge. For this study we used two different density distributions to represent the dark halo. First we used a spherical distribution given by an isothermal sphere with a density profile given by:

$$\rho = \frac{\rho_0}{[1 + (\frac{r}{r_0})^2]^{3/2}} \tag{3}$$

where ρ_0 is the central halo density and r_0 the core radius. We also used the Navarro, Frenk and White (Navarro, Frenk & White 1996) (hereafter NFW) density profile:

$$\rho = \frac{\rho_0}{\frac{r}{r_0}(1 + \frac{r}{r_0})^2} \tag{4}$$

The result of the quadratic sum of each velocity component (bulge, disk and halo) is fitted to the observational rotation curve by minimizing the reduced [6] χ^2 in the four dimensions space: $(M/L)_{disk}$, $(M/L)_{bulge}$, ρ_0 and r_0. The reduced χ^2 can be affected by small and large scale variations in the measured velocities that can have various origins (bars, other non-aximmetric motions, star formation, projection effects, etc) that the models does not take into account. A high χ^2 does not therefore necessarily means a bad fit. A reduced χ^2 around 1 is an indication of a good fit, but because of the degeneracies between parameters the result may not be unique. We looked if errors listed in table 1 and 2 for the halo and M/L parameters are correlated with the reduced χ^2. It appears that the reduced χ^2 remains more or less constant with the errors, showing no correlations. In appendix (A) we give comments on each galaxy analysis. In appendix (B) (from figure 4 to figure 21) we present the fits to the J-band surface brightness profiles and the rotation curves using the isothermal sphere to model the dark halo. The velocity uncertainties, presented on the plots, are the differences between the two sides of the rotation curve (receeding and approaching). In appendix (A) we also give a description of the fit for both the NFW and maximum disk hypothesis for the dark halo, but the corresponding plots are not presented in the paper.

---

[5] IRAF is distributed by the National Optical Astronomy Observatory, which is operated by the Association of Universities for Research in Astronomy (AURA) under cooperative agreement with the National Science Foundation

3. COMPARISON SAMPLES OF FIELD AND CLUSTER GALAXIES

The main goal of this work is to compare the mass distributions for galaxies in dense environments with the ones found in less dense or isolated environments. Two different works can be found in the literature to which we could compare our results: Barnes et al. (2004) (hereafter B04) studies on galaxies in clusters and Spano et al. (2008) (hereafter S08) studied field galaxies.

3.1. *Cluster Galaxies - B04*

B04 shows rotation curves for 40 spiral galaxies from the Schommer et al. (1993) survey, observed with a FP interferometer. B04 followed a similar technique to ours using both the photometry (in the I-band) and the RCs in order to fit the halo parameters and determine the mass distribution. The photometric profiles used by B04 come from Palunas et al. (2000). Two dark halo models were used by B04, same as those used by us, a pseudo-isothermal and the NFW density profile. The sample from Schommer et al. (1993) is not very homogenous with respect to galaxy environment. More than half the galaxies present comes from clusters. In order to compare our results with cluster galaxies, we had to convert the NFW dark halo parameters they used into our set of parameters. We deduced the central density (ρ_0) and the core radius (r_0) from the v_{200} and c from B04 using definitions found in NFW. The parameters for the iso-thermal halo are the same as ours. B04 found that stars-only model fits most of the RCs of their sample over a significant radial range. But the addition of a dark halo generally leads to low values of M/Ls. They also confirm a scaling law between the central halo density and the core radius. Palunas et al. (2000) used I-band photometry and the M/L indicated in B04 were determined in the same band. In order to compare the results from our sample with the cluster galaxies, it was necessary to transform our surface brightness profile from the J-band to the I-band. We first made the hypothesis that the profile in the J-band has the same shape and slope as in the I-band (same scale length for the exponential disk and same r_e for the bulge).

Only the μ_0 and μ_e were modified. We used the apparent magnitude found in NED [7] in the SDSS i-band for our galaxies and determined the absolute magnitude in the Johnson I-band using Fukugita et al. (1995) formula and the distances noted in the RC3 (de Vaucouleurs et al. 1991). We scaled the surface brightness profile of our galaxies in order to get the calculated I-band absolute magnitude using our mass model program. Hereafter we perform the comparison with all the cluster galaxies sample from B04 and our HCG galaxies and we discuss the results in the conclusion but we did not plot it in the paper.

3.2. *Field Galaxies - S08*

We also wanted to compare with the field galaxies from the GHASP survey (Galaxies HAlpha Survey Project, Garrido et al. (2002), Garrido et al. (2003), Garrido et al. (2004), Garrido et al. (2005), Epinat et al. (2008a), Epinat et al. (2008b)) where late-type field galaxies have been observed using a Fabry-Perot interferometer. S08 present the mass model for a sub-sample of 36 galaxies of the GHASP survey. For this survey, we had to convert our J-band surface brightness profiles into R-band. For HCG 16a, HCG 88a, HCG 88c, HCG 89a and HCG 89c, we directly used the surface brightness profiles from Rubin et al. (1991) and for HCG 96c we used the profile from Verdes-Montenegro et al. (1997). We estimated a mean shift between μ_0 in the J-band and μ_0 in the R-band for the remaining galaxies and we verified that the M_R magnitudes obtained with the mass model program were consistent with what we found in the litterature (Hickson et al. 1989). S08 confirm the halo scaling laws showing that low luminosity galaxies have small core radius and high central halo density and that the halo surface density is constant with the absolute magnitude. They also found that a trend can be seen between the core radius and the color or the disk scale length.

The galaxies from the cluster galaxies sample have absolute B magnitudes between: $-21.5 < M_B < -19.0$ and the field galaxies B magnitudes are between $-22.0 < M_B < -15.5$. Our sample of HCG have $-21.5 < M_B < -18.5$. We performed a KS test between our sample and the cluster galaxies sample plus a sub-sample of the field galaxies with an $M_B < -18.5$ representing 16 galaxies. The results show they are similar at the 85% level or higher. We then used this sub-sample of the field galaxies sample with $M_B < -18.5$ to perform the comparison.

4. MASS DISTRIBUTION IN GALAXIES IN COMPACT GROUPS: COMPARISON WITH FIELD AND CLUSTERS GALAXIES

In this section we discuss the relationships between halo parameters, disk M/L ratios, halo and disk masses using the different halo models and also comparing with other galaxies samples (figures B1 to B3).

---

[6] The reduced χ^2 is the χ^2 divided by the number of degrees of freedom.

[7] NASA/IPAC Extragalactic Database (NED) which is operated by the Jet Propulsion Laboratory, California Institute of Technology, under contract with the National Aeronautics and Space Administration

In order to point out differences in the halo shape parameters between galaxies in different environment, we compared the two samples, cluster and field galaxies, using both the ISO and the NFW dark halo profiles.

Thus we analyse the disk M/L and the halo mass fraction as a function of the B absolute magnitude (see figure **??**) and we compare the halo mass fraction and the disk M/L using a ISO or a NFW halo (see figure B3).

We only compare with field galaxies and we derived the M/L within the R-band. For the halo central density and the core radius, we estimated the errors of the fit by taking the 1σ error of the χ^2 minimization. We plot the maximum error bars determined for different figures in order not to overfill the plots.

Finally we show differences between the central halo density and core radius using ISO and NFW halo models and we compare the χ^2 for those two halo models (figure B3).

4.1. *Halo parameters*

In order to make a fair comparison of the halo parameters, we evaluated these parameters using the R and I photometry for the HCG galaxies. Coefficients of the linear regression are quite similar and differences are inside the error bars of the linear fit. For this reason we present in figure B1, the halo parameters derived using the J-band photometry.

4.1.1. *Central halo density versus core radius (ρ_0 vs r_0)*

Figures B1a,b show the tight correlation between the central halo density ρ_0 and the core radius r_0 using the ISO and NFW models for galaxies in three different environments. Figure B1a shows the strong correlation between the central density and the core radius for all samples using the ISO model. Table 3 summarises coefficients of the linear regression with the correspondent correlation coefficients.

These fits were obtained excluding 5 galaxies from the cluster galaxies sample because they were several orders of magnitude out of range. For the cluster galaxies sample, 5 galaxies show highly peaked halos in comparison with the other galaxies. Cluster galaxies galaxies show that part of the sample has lower core radii, when compared to HCG and field galaxies. This is mainly due to the fact that B04 uses a pseudo-isothermal halo density profile instead a strict isothermal model. With the MDM model (not shown on the plot), the relation is also very well defined with a correlation of:

$Corr = -0.70 \pm 0.26$ (see table 3).

Figure B1b shows the same correlation as before but using NFW model. It is clear that the relation between the central halo density and the core radius is much scattered using the NFW than the ISO model.

The correlation found using the NFW model is $Corr = -0.48 \pm 0.46$ for the HCG galaxies and the central density of the regression is lower than the ISO model. The correlation between the central halo density and the core radius is very strong for the three samples using ISO or NFW models. The correlation coefficient is almost the same for the cluster galaxies sample using either the ISO or the NFW models and quite different for the field and HCG samples using these two models.

4.1.2. *Disk scale length and halo core radius versus absolute B magnitude (h and r_0 vs M_B)*

Instead of plotting the disk scale length versus halo core radius as S08 and Kormendy (2004), we present the disk scale length normalised to the halo core radius vs the absolute magnitude. The result is presented in figure B1c. We used the all field galaxies sample in order to display the less luminous galaxies. For the field galaxies it is clear that the ratio is constant, showing that the core radius and the disk scale length are connected somehow and that it is independent from galaxy luminosity. The result for the three samples is consistent. We perform the plot using the ISO model only, but the result is almost the same if we use NFW. From Freeman (1970) and Parodi et al. (2002) we know that the disk scale length is proportional to the galaxy luminosity for a large variety of galaxy types. This relation is also found for field and HCG galaxies. We verified that the core radius increases with the galaxy luminosity.

4.1.3. *Halo surface density versus absolute magnitude ($\rho_0 * r_0$ vs M_B)*

In Figure B1d, we present the halo central surface density ($M_\odot.pc^{-2}$) versus the B absolute magnitude for the three samples using the isothermal sphere. HCG galaxies from our sample are brighter than the field galaxies, but the halo surface density is almost the same between the three samples using the ISO model. S08 found, from the central halo density and the core radius as a function of the absolute magnitude, that faint galaxies show a more concentrated dark halo than massive late type galaxies. S08 confirmed the results of Kormendy (2004), with a slightly higher constant halo density. However, with the cluster galaxies sample and our HCG galaxies, it is difficult to confirm this trend because of the lack of faint galaxies in both samples. The results using NFW model are very similar to what can be observed with ISO.

Romano-Díaz et al. (2007) have investigated the evolution of galactic dark matter haloes through collisionless high resolution N-body simulations. They found that haloes evolve through a series of quiescient phases, well fitted by a NFW profile. They showed that the characteristic density ρ_s and the radius r_s are strongly correlated.

4.2. *Disk mass-to-light ratio*

In this section, we discuss the fitted disk M/L parameter using the ISO, the NFW models (see figure B2a and B3a).

The dependence of disk M/L on the absolute magnitude for both samples (field and HCG galaxies) is analysed in figure B2a using only the ISO model. More than half the HCG galaxies show a very low disk mass-to-light ratio (inferior to one). If we limit the field galaxies sample to galaxies with similar magnitudes ($M_B < -18.5$), we found that slightly less than half field galaxies have disk M/L larger than 4.0 when the maximum M/L for HCG galaxies is 3.9. *HCG galaxies have a lower M/L disk ratio than isolated galaxies in the same range of absolute blue magnitude.* This may be due to galaxies in Hickson groups having luminosities boosted by star formation triggered by interactions or their maximum velocities diminished by tidal stripping.

The disk mass-to-light ratio between ISO and NFW halo models for both the HCG galaxies and the field galaxies of GHASP are analysed in figure B3a. We first can notice that M/L values for the HCG galaxies are spread over a large range. This situation is clearer for field galaxies. Almost all galaxies show a greater M/L using the ISO model. (a) With HCG 87a, the NFW model can't fit the rotation curve with a minimum of halo and a little disk, while ISO puts the disk to almost zero and extend the dark halo. (b) For HCG 91c, NFW puts the bulge to zero and gives a larger disk than ISO. The result is that the central part is better fitted with ISO and the outer part of the rotation curve is better using NFW and the χ^2 is very similar for both. (c) The situation is similar with HCG 007c because of a bump that neither model can fit. The fact that NFW gives lower M/L disk ratios is consistent with what B04 found for their sample. In their case, the photometry was done in I-band, but it does not change significantly the trend.

We also compared the disk M/L for HCG between ISO and the maximum disk model (not shown here). The agreement is high even if MDM has, by definition, a natural tendency to give an higher disk M/L. This means that the BFM gives a solution that is very close to MDM and thus MDM appears to be the favourite solution.

In conclusion, using the ISO model instead of the NFW model results in a greater disk M/L and that, at least for HCG galaxies, the disk mass is independent of the galaxy luminosity.

4.3. *Halo and disk masses*

This section presents relations between halo and disk masse as a function of absolute magnitude for two different models: ISO and NFW. Table 4 presents the disk mass, halo mass and halo mass fraction using the different models ISO, NFW and MDM. In the determination of the total mass, the HI mass was not taken into account.

Figure B2b shows the halo mass fraction versus the absolute magnitude for both HCG and field galaxies. The plot shows that only three HCG galaxies, HCG 10d, HCG 96c and HCG 88a, have a halo mass fraction lower than 0.8 within the range of absolute B magnitude and 66% of field galaxies have halo mass fraction larger than 0.8 for a larger range of B magnitude. This can be explained by the fact that the disk is predominent. The others galaxies (HCG and isolated galaxies) are totally dominated by the dark halo and the dark halo is not related to the luminosity of the galaxy.

We were interested in a possible relation between M_{Disk}/L_B and the disk mass for HCG and field galaxies. Figure B2c shows a clear correlation between the disk M/L_B and the disk mass for both HCG and field galaxies. As for all figures in that section, we have plot the all sample of field galaxies, if we restrict the field galaxies sample to those with an absolute B magnitude inferior to -18.5, we noticied that HCG galaxies and field galaxies follow the same relation.

This is confirmed with a work by Salucci et al. (2008) that analyse disk masses for 18 spirals by both modelling their rotation curve and by fitting spectral energy distributions. The authors found a good agreement between the two methods. Beside their discussion about the best way to calculate the disk mass, they present the relationship between the stellar mass, the color and the stellar mass-to-light ratio. They found that the M/L is increasing with the disk mass.

Based on a technique of mass decomposition of spiral galaxies from disk kinematics (Persic & Salucci 1990), found that the ratio of the disk mass to halo mass fraction shows a strong dependency with respect to the luminosity. Their study points out a higher disk mass compared to our sample or field galaxies.

Figure B3b compares the relation between the ratios halo mass fraction / total mass estimated with ISO and NFW models for both HCG and field galaxies. A KS test between the two halo mass fractions from field and compact group galaxies for the same range of absolute B magnitude, proved that both samples have 90% chance to be drawn from the parent distribution, indicating that there is no statistical difference between the two Four galaxies (HCG 007c, HCG 10d, HCG 87c and HCG 91c) show lower halo masses using the NFW profile. The halo is much more important for HCG 007c using the ISO model with respect to NFW, but both fit shows a poor χ^2. Even if HCG 87c does not show a disturbed RC, NFW halo model provides a poor fit. No fit is possible to mimic the rotation curve with a NFW halo model. For HCG 91c, both models lead to almost the same amount of disk, but NFW uses 10 times less halo than ISO for almost the same χ^2.

In conclusion, for both field and HCG galaxies, the mass is dominated by the halo, as B04 showed, and no differences are found between galaxies in the field and galaxies in dense environment with respect to disk mass.

4.4. *Isothermal model versus NFW halo profile*

We have compared the halo parameters (core radius and central density) for both models (NFW and ISO) for both HCG and field galaxies. Figures B3c,d show that the central halo density with ISO is higher than NFW and, in the mean time, the halo core radius is smaller with ISO than with NFW. The isothermal model gives apparently a more concentrated dark halo shape than the NWF96 model. This seems in contradiction with the "natural" cuspy shape of NFW dark halo profile. Indeed ISO profile is shallow in the center while NFW is more peaked. (see Blais-Ouellette (2000) for the comparison between the two halo profiles). The different parameters of the halo ρ_0 and r_0 are derived together with the M/L of the disk using the best fit model on the RCs. Since the slope of the RC is not high enough to be fitted by the cuspy NFW profile, it favours the disk and thus underestimates the halo. This is not the case with the core - like ISO model which matches the relatively faint slope of the RC and thus minimizes the disk and favours the halo.

Figure B3e compares the quality of the fits using a χ^2 parameter between the isothermal sphere and the NFW models for both HCG and field galaxies. To display the result, we have limited the χ^2 range between 0 and 15. Two galaxies (HCG 19a and HCG 91a) show a high χ^2 (> 30) with both models. Two galaxies (HCG 087c and HCG 88d) show a very poor χ^2 with the NFW model only. Three other galaxies (HCG 16c, HCG 19b and HCG 89c) show a higher χ^2 for the NFW than for the isothermal sphere. S08 noted that NFW gives higher χ^2 than the ISO model. Figure B3e confirms this for HCG galaxies.

We can conclude that, as for field galaxies, HCG ISO dark halo fits the RC better than the NFW model.

5. SUMMARY AND CONCLUSIONS

Based on a sample of $\approx$ 100 velocity fields of spiral galaxies belonging to 25 HCGs, our previous study has demonstrated that: 40% (38 galaxies) of the HCG galaxies analysed in our sample do not allow the computation of the RC. This is because these galaxies are strongly perturbed by interaction and mergers. 33% (31 galaxies) of HCG galaxies are regular enough to calculate a RC but the RC is not symmetric to allow the derivation of a mass model. These perturbed galaxies are mildly interacting. The remaining 27% (25 galaxies) of them are suitable to derive mass models. For a variety reasons only 18 galaxies have been studied in the present work. The RCs have been combined with 2MASS J-band surface brightness profiles to derive their mass models. Two shapes of dark halos have been considered: a core-like density profile (isothermal sphere or ISO) and a cuspy-like one (NFW). Best fit models and maximum disk models have been computed for the two dark halo profiles. We have compared the HCG galaxies with two samples of galaxies in different environments: field and clusters galaxies. The three samples (HCG, isolated and cluster) have been analysed using the same tools.

The results are summarized below:

- No obvious differences can be found between the halo parameters for the HCG galaxies and galaxies in other environments. The strong correlation between ρ_0 and r_0 is present for the three samples and the slopes of the linear regressions between them are very similar (between -1.62 and -1.00), well inside the uncertainties. In a study based on late-type and dwarf spheroidal galaxies, Kormendy (2004) confirms this correlation giving a slope of -1.038. On the other hand, the linear regression constant found by Kormendy (2004) is different in comparison with those found with the three samples. This scale difference is may be due to the fact that Kormendy (2004) compiled his sample using several sources using different methods to obtain halo parameters.

- The use of the NFW model gives less satisfactory results than the ISO model. As mentioned by S08, the χ^2 coefficient is usually larger when using the NFW. NFW model gives a worse correlation between the halo central density and the core radius than ISO. This is also true if we use the field galaxies sample. In contrast, the NFW model gives a consistent result for the cluster galaxies sample. Halo profiles are closer to isothermal spheres than NFW profile as already found by other authors (Blais-Ouellette et al. 2001; de Block & Bosma 2002; Swaters et al. 2003; Kassin et al. 2006; Spano et al. 2008). The slope of the linear regression between ρ_0 and r_0 is higher for thecluster galaxies sample than for the two other samples when the NFW model is used. The disagreement between ISO and NFW is smaller with cluster galaxies sample. 61% of HCG galxies shows higher disk M/L using the ISO model compared to NFW. No relation between the disk scale length and the halo central density is seen using either ISO or NFW models.

- We explored the possible connection between the halo parameters, the halo mass fraction and the disk M/L. The halo mass is high for both field galaxies and compact groups galaxies (75 to 95% of the total mass), leaving only modest room for the disk mass. The halo surface density is independent of the absolute B magnitude and no clear relation is seen between the disk M/L and M_B, meaning that the halo is independent of the galaxy luminosity.

Because of the lack of low luminosity HGC galaxies, we could not investigate properl the possible relation between the disk scale length and the halo core radius as S08 and Donato et al. (2004). We just can say that, for our sample of bright HCG galaxies ($M_B < -18.5$) no clear trend could be found.

HP would like to thank the Scientific Council of the Laboratoire d'Astrophysique de Marseille (LAM) for its financial support during the visits in February 2007 and 2008. HP thanks the CAPES foundation for its financial support during HP fellowship at LAM during the year 2009 (process 3656/08-0). HP would like to thank Dr. D. Russeil for its help in the surface brightness decomposition. HP wishes to thank Niraj Welikala for the English proof reading of this paper. The authors wish to thank the anonymous referee for its comments. This research has made use of the NASA/IPAC Extragalactic Database (NED) which is operated by the Jet Propulsion Laboratory, California Institute of Technology, under contract with the National Aeronautics and Space Administration. This publication makes use of data products from the Two Micron All Sky Survey, which is a joint project of the University of Massachusetts and the Infrared Processing and Analysis Center/California Institute of Technology, funded by the National Aeronautics and Space Administration and the National Science Foundation.

REFERENCES

Amram, P., Plana, H., Mendes de Oliveira, C., Balkowski, C., Boulesteix, J. 2003, A&A, 402 , 865
Amram, P., Mendes de Oliveira, C., Plana, H., Balkowski, C., Hernandez, O., Carignan, C., et al., 2004 ApJ, 612, L5
Amram, P., Mendes de Oliveira, C., Plana, H., Balkowski, C., Hernandez, O. 2007, A&A., 471, 75
Barnes E.I., Sellwood J.A., Kosowsky A. 2004, AJ, 128, 2724
Blais-Ouellette S., 2000, Ph.D. Thesis, Université de Montréal.
Blais-Ouellette S., Amram P., Carignan C., 2001, AJ, 121, 1952.
Carignan, C., Freeman, K.C. 1985, ApJ, 294, 494
Casernato, S. 1983, MNRAS, 203, 735
de Block W.J.G. & Bosma A., 2002, A&A, 385, 816
de Vaucouleurs, G.; de Vaucouleurs, A.; Corwin, H. G.; Buta, R. J.; Paturel, G.; Fouque, P. VizieR On-line Data Catalog: VII/155. Originally published in: Springer-Verlag: New York, (1991), Third Reference Cat. of Bright Galaxies (RC3)
Donato F., Gentile G., Salucci P., 2004, MNRAS, 353, L17.

Durbala, A., del Olmo, A., Yun, M. S., Rosado, M., Sulentic, J. W., Plana, H., Iovino, A. et al. 2008, AJ, 135, 130

Epinat, B.; Amram, P.; Marcelin, M.; Balkowski, C.; Daigle, O.; Hernandez, O.; Chemin, L.; Carignan, C.; Gach, J.-L.; Balard, P. 2008 MNRAS, 388, 500

Epinat, B.; Amram, P.; Marcelin, M. 2008 MNRAS, 390, 466

Fletcher, R. 1970, Comp. J., 13, 317

Freeman, K.C. 1970, ApJ, 160, 811

Fukugita, M., Shimasaku, K., Ichikawa, T. 1995, PASP, 107, 945

Garrido O., Marcelin M., Amram P., Balkowski C., Gach J.L., Boulesteix J. 2005, MNRAS, 362, 127

Garrido O., Marcelin M., Amram P., 2004, MNRAS, 349, 225

Garrido O., Marcelin M., Amram P., Boissin O., 2003, A&A, 399, 51

Garrido O., Marcelin M., Amram P., Boulesteix J., 2002, A&A, 387, 821

Hickson, P., Kindl, E., Auman, J.R. 1989, ApJS, 70, 687

Hickson, P., Mendes de Oliveira, C., Huchra, J.P., Palumbo, G. 1992 ApJ, 399, 353

Kassin, Susan, A., de Jong, Roelof S., Weiner, Benjamin, J. 2006, ApJ, 643, 804

Kormendy J., Freeman K.C. 2004, IAU Symposium 220. S. Ryder, D.J. Pisano, M. Walker & K.C. Freeman editors, p. 377

Mendes de Oliveira, C., Plana, H., Amram, P., Bolte, M., Boulesteix, J. 1998 ApJ, 507 691

Mendes de Oliveira, C., Plana, H., Amram, P., Balkowski, C., Bolte, M. 2001, AJ, 121, 2524

Mendes de Oliveira, C., Amram, P., Plana, H., Balkowski, C. 2003, AJ, 126, 2635

Navarro, J.F., Frenk, C.S., White, S.D. 1996, ApJ, 462, 563

Palunas P., Williams T.B. 2000, AJ, 120, 2884

Parodi, B. R., Barazza, F. D., Binggeli, B. 2002, A&A, 388, 29

Persic, M., Salucci, P. 1990, MNRAS, 245, 577

Plana, H., Mendes de Oliveira, C., Amram, P., Boulesteix, J. 1998, AJ, 116, 2123

Plana, H., Mendes de Oliveira, C., Amram, P., Bolte, M., Balkowski, C., Boulesteix, J. 1999 ApJ, 516, L69

Plana, H., Amram, P., Mendes de Oliveira, C., Balkowski, C. 2000, AJ, 120, 621

Plana, H., Amram, P., Mendes de Oliveira, C., Balkowski, C., Boulesteix, J. 2003, AJ, 125, 1736

Plana, H., Amram, P., Balkowski, C., Mendes de Oliveira, C. *Galaxies: The Third Dimension*, ASP Conference Proceedings, Vol. 282. Edited by Margarita Rosado, Luc Binette, and Lorena Arias. San Francisco: Astronomical Society of the Pacific, 2002., p238

Romano-Díaz E., Hoffman Y., Heller C., Faltenbacher A., Jones D., Shlosman I., 2007, ApJ, 657, 56

Rubin V.C., Hunter D.A., Ford W., Kent Jr. 1991, ApJS, 76, 153

Salucci P., Yegorova I.A., Drory N. 2008, MNRAS, 388, 159

Schommer R.A., Bothun G.D., Williams T.B., Mould J.R. 1993, AJ, 105, 97

Spano M., Marcelin M., Amram P., Carignan C., Epinat B., Hernandez O., 2008 MNRAS, 383, 297

Skrutskie, M.F., Cutri, R.M., Stiening, R., Weinberg, M.D., Schneider, S., Carpenter, J.M., Beichman, C. et al. 2006, AJ, 131, 1163

Swaters R.A., Madore B.F., van der Bosch F.C., Balcells M., 2003, ApJ, 583, 732

Torres-Flores, S., Mendes de Oliveira, C., de Mello, D., Amram, P., Epinat, B., Plana, H. and Iglesias-Páramo, J. 2009, A&A, submitted

Verdes-Montenegro, L., del Olmo, A., Perea, J., Athanassoula, E.; Marquez, I., Augarde, R. 1997 A&A 321, 409

Zhao H., 1996 MNRAS, 278, 488

APPENDIX

COMMENTS ON INDIVIDUAL GALAXY

HCG07c: HCG07 is composed of four galaxies (Hickson et al. 1992). We only analyse the kinematics of HCG07c, a galaxy with morphological type SBc. The rotation curve rises to a velocity of about 170 km/s, at a radius of r $\sim 35''$(10 kpc) and then goes down to a plateau, at a lower velocity of $\sim$ 150 km/s, out to a radius of $52''$(14.5 kpc). At small radius, the curve is not regular: a plateau is present between $5''$(1 kpc) and $8''$(2 kpc). Because of the irregularity of the RC, the fit is not good, especially in the center. The bulge component is rather significant in the fit, in order to take into account the first $5''$(1 kpc) of the curve. The halo has, by far, the largest contribution of the fitted RCs. It reaches a plateau at $\sim 35''$(10 kpc). The disk, on the other hand, is weak and its contribution is no more than 10% of the total rotation velocity.

When using NFW model and the maximum disk hypothesis, we found a more prominent disk and the halo shows a plateau around $20''$(6kpc).

The photometric profile is well fitted with a bulge and an exponential disk. Note that the disk profile presents wiggles (most probably due to the spiral arms). In addition, the fit of the bulge within the first $4''$(0.8 kpc) is not good, as can be seen from the well visible deviations in figure 1.

HCG10d: HCG10 is composed of four galaxies. We applied the mass model to HCG10d, an Sc-type galaxy. The rotation curve rises regularly to 149 km s^{-1}, out to $20''$(6 kpc). No bulge has been used to fit the RC. The fit is very good and both the disk and the halo almost have an equal contribution in the RC. The halo shows a plateau around $10''$(3 kpc) and its contribution is more regular than the disk. As for the NFW and maximum disk models, the contribution for the disk is larger than for the isothermal halo. In particular, in the case of NFW, the disk is responsible for almost 90% of the velocity of the RC.

The photometric profile shows that an exponential disk alone is enough to fit it.

HCG016a: HCG16 is a group formed of four galaxies. HCG16a is an SBab type galaxy. The rotation curve is a typical example of a late-type rotation curve with a sharp rise in the first $4''$(3 kpc) till the maximum rotation velocity of 247 km.s^{-1} and a plateau reaching out to $30''$(8 kpc). The general fit is good (ignoring the wiggles in the profile due to the spiral arms). The bulge has the largest contribution for any single galaxy in our sample. The contribution of the halo and the disk are comparable, except for the fact that the halo reaches a constant value around $\sim 14''$(3.5 kpc) at 140 km s^{-1} and the disk rises constantly.

The use of the NFW model for the dark halo shows a much larger contribution for the halo (more than 65% of the fitted RC) with a plateau starting at $8''$(2 kpc). The maximum disk model gives a larger contribution of the disk (as expected) and the halo represents only 30% of the maximum rotational velocity.

The photometric profile shows that the disk profile suffers a drop starting at $22''$(5.5 kpc), below the theoretical exponential disk. In that case, for the mass model we used a theoretical exponential disk from $2''$(0.5 kpc) to $30''$(8 kpc).

HCG016c: HCG16c is an S0 galaxy. The rotation curve is slowly rising to 200 km s^{-1}. The fit of the rotation curve does not fit well an observed depression between $10''$(2 kpc) and $22''$(5 kpc), but the rotation curve is almost entirely dominated by the halo, except the first $5''$(1.2 kpc), where the disk and the bulge allow a good fit

The result is almost identical for the other two models we used. The halo totally dominates the RC.

The photometric profile is well fitted by a rather important bulge and an exponential disk. In this case the wiggles are probably not related to spiral arms but instead with the merger nature of this galaxy Mendes de Oliveira et al. (1998).

HCG19a: HCG19 is a group formed of four galaxies and its brightest member, HCG 19a, is an S0 galaxy. The rotation curve of this galaxy shows a flat part within a radius of $2''$(0.5 kpc) and a rise outward, reaching a velocity of 125 km s^{-1} at $20''$(5.5 kpc). The fit is rather poor and only the halo has a contribution. No disk has been used to fit the RC.

The other two models do not fit the rotation curve any better. In particular, the NFW model is a very poor fit to the data, since it cannot reproduce the maximum velocity at $35''$(9.5 kpc).

The photometric profile is well fitted with only a bulge contribution.

HCG19b: HCG19b is classified as an Scd galaxy and its rotation curve is quite irregular. It presents a small plateau between $6''$(1.8 kpc) and $12''$(3 kpc). It then reaches a maximum velocity of 90 km s^{-1} at around $30''$(8 kpc). Due to these irregularities, the fit of the rotation curve is not good. The halo is the major contribution of the rotation curve and the disk has only a contribution of 20% of the total rotational velocity.

The results of the fit using the two other models are better. In these case the contribution of the halo is more important than using the ISO model.

The photometric profile shows a drop at $12.5''$(3.2 kpc). We replaced the part of the profile between $12.5''$(3.2 kpc) and 30 $''$(8 kpc) by an exponential disk.

HCG87a: HCG87 is a group formed of three galaxies, and its brightest member, HCG87a is an Sbc galaxy. The rotation curve shows a solid body rotation with rotational velocity rises up to 400 km s^{-1} at $25''$(13 kpc). This is certainly due to the fact that this object is almost edge on.

Fits of the RCs with the two others models show that the largest contribution comes from the disk, but the fits are not as good as with the isothermal halo. In both cases the halo does not represent more than 45% of the total rotational velocity.

The photometric profile is not well fitted by an exponential between 12″(6 kpc) and 26″(14 kpc) where a bump is present.

The first 7″(3.5 kpc) of the profile are well fitted by a bulge profile.

HCG87c: HCG87c is classified as an Sd galaxy. The rotation curve is regular and shows a plateau at 10″(5.5 kpc) with a maximum velocity of 160 km s^{-1}. The halo fits almost completely the RC. No bulge is present and the disk shows a plateau beginning at 6″(3.5 kpc).

The result of the fit using the maximum disk is the same as for the isothermal halo. On the other hand, the fit using the NFW model is very poor and cannot reach the maximum velocity.

The photometric profile is fit only with an exponential disk.

HCG88a: HCG88 is formed of four galaxies, and its brightest member, HCG88a is classified as an Sb galaxy. The rotation curve rises regularly without reaching a plateau. The disk contribution is prominent. The halo contribution rises linearly and the bulge contribution fits well the beginning of the curve. The fit of this rotation curve is one of the best of our sample.

The two other models show a very good fit of the rotation curve but the NFW model indicates a larger contribution of the halo (∼ 38%) in comparison with the isothermal halo. The disk contribution is lower in, almost, the same proportion.

The photometric profile is very well fitted with a bulge and an exponential disk.

HCG88b: HCG88b is an SBb galaxy. The rotation curve rises regularly. It presents a small plateau between 4″(1.5 kpc) and 10″(4 kpc) and between 30″(11.5 kpc) and 40″(15.5 kpc). The rotation curve rises to 300 km s^{-1} and then drops to 190 km s^{-1}. Due to these irregularities, the ”best fit” is clearly not appropriate. The largest contribution comes from the disk. It shows a plateau at 210 kms s^{-1}. The bulge also has a large contribution in order to fit the inner part of the curve and the halo rises linearly to 190 km s^{-1}.

The result of the fit using the NFW model shows a major contribution of the halo and the result for the maximum disk is almost identical to that of the isothermal halo.

The photometric profile is well fitted by a combination of a bulge an exponential disk. However the disk shows some small oscillations which obviously cannot be reproduced with an exponential disk.

HCG88c: HCG88c is classified as an Scd galaxy. The rotation curve reaches a maximum velocity of 130 km s^{-1}. The fit performed using only the halo and disk contributions is good. The halo rises regularly and the disk profile shows an unusual shape. The disk profile shows two peaks, at 7″(2.5 kpc) and 15″(5.8 kpc), and a small depression in between.

The maximum disk shows a similar result to that given by the isothermal halo model. The fit with the NFW model shows that the halo alone can almost account for the whole RC. The disk has only a marginal contribution.

We tested the fit of the rotation curve using a theoretical exponential but this fit did not represent well the depression of the rotation curve at small radii, we decide then to keep photometric profile.

HCG88d: HCG88d is classified as an Sm galaxy. The rotation curve rises regularly without showing any plateau, out to a radius of 30″(11 kpc). The fit with a halo and an exponential disk contributions is very good. The halo rises linearly and the disk rises to a maximum, at 12″(4.5 kpc) and then slowly decreases. The maximum disk model presents similar results to that given by the isothermal sphere, but the NFW model is not able to fit the curve at all.

The photometric profile is very well fitted with only a disk.

HCG89a: HCG89a is classified as an Sc galaxy. The rotation curve shows a bump between 4″(2 kpc) and 8″(4 kpc) and then the velocities rise regularly up to 220 km s^{-1}.

This bump can not be fitted with a larger contribution from the bulge without spoiling the fit of the curve beyond 10″(5 kpc).

The halo profile is increasing almost linearly. The disk contribution rises to 90 km s^{-1} and then slowly decreases. We could not fit properly the entire curve even using an exponential disk instead of the original disk photometric profile. The maximum disk model gives similar results even if the bump present between 4 and 8″is not as well fitted. The NFW model shows that the halo alone is responsible for almost the whole RC, but the model fails to take the bulge into account.

The photometric profile is well fitted with a bulge and an exponential disk, for radii up to 12″(6 kpc), after which the profile drops.

HCG89b: HCG89b is an SBc galaxy. The rotation curve shows a plateau starting at 6″(3.2 kpc), with a maximum velocity of 120 km s^{-1}. The halo presents the largest contribution, showing a plateau also around 6″(3.2 kpc). The NWF96 model and the maximum disk basically yield the same result.

We replaced the photometric profile between 0 and $6''$(3.2 kpc) and with a theoretical exponential disk, to obtain the disk contribution of the RC. We tested the fit of the rotation curve using the original brightness profile, but the fit is not significantly different.

The surface brightness profile is well fitted using an exponential disk profile except for the first $6''$(3.2 kpc) where the profile is flat. This is certainly due to an apparent double nucleus, present on the 2mass and DSS images.

HCG89c: HCG89c is an Scd galaxy. The fit is very good with a larger contribution of the dark halo in comparison with the disk. The use of the maximum disk does not show much of a difference in the result of the fit. The NFW fit, on the other hand, yields the worse fit. In that case the halo occupies almost the entire fitted RC.

As for HCG89b, the photometric profile is fitted with an exponential disk only, except at the very beginning, where the profile is flat.

HCG91a: HCG 91 contains four galaxies, the brightest being, HCG 91a, classified as an SBc galaxy. The rotation curve for this galaxy is very irregular and, in particular, for a radius greater than 20 $''$(9 kpc), the rotation curve is very asymmetric. The major contribution comes from the bulge, the disk contribution being much less important. The halo presents a plateau at $10''$(4 kpc). The NFW model gives an even larger contribution from the bulge and the disk is marginal. The maximum disk model yields similar results to those given with the isothermal halo.

The photometric profile is well fitted with a bulge and an exponential disk.

HCG91c: HCG91c is classified as an Sc galaxy. The rotation curve is regular, with a plateau at $16''$(7 kpc), and with a velocity of about 120 km s^{-1}. The fitted rotation curve is completely dominated by the disk. The halo only represents 30% of the total rotation velocity and the bulge contribution is marginal. The fit with the NFW hardly uses a dark halo and for the maximum disk model the result is similar to that for the isothermal halo, only with an even higher disk contribution.

The photometric profile is well fitted by a large bulge and an exponential disk. Since at $13.5''$(6 kpc) the profile drops drastically, we replaced this part with a theoretical exponential disk to derive the disk contribution for the RC.

HCG96c: HCG96c, one of the four galaxies of the compact group HCG 96, is classified as an Sa. Its rotation curve is not very extended. It shows a plateau at $4''$(2.2 kpc), with a velocity of 80 km s^{-1}. No bulge was used, the halo rises linearly and the disk has the largest contribution to the RC. The result of the fit using the maximum disk is similar and the fit using the NFW model shows a larger contribution of the dark halo (of about $\sim 15\%$) in the first $4''$(2 kpc). After which the halo increases at a slower rate.

The photometric profile is well fitted with a disk and a very small bulge, except at the outskirts of the galaxy.

SURFACE BRIGHTNESS PROFILES AND ROTATION CURVES

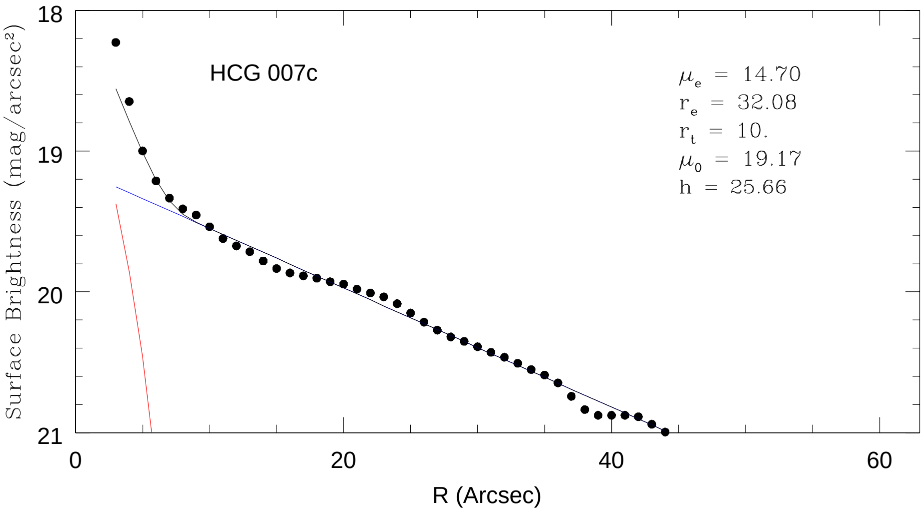

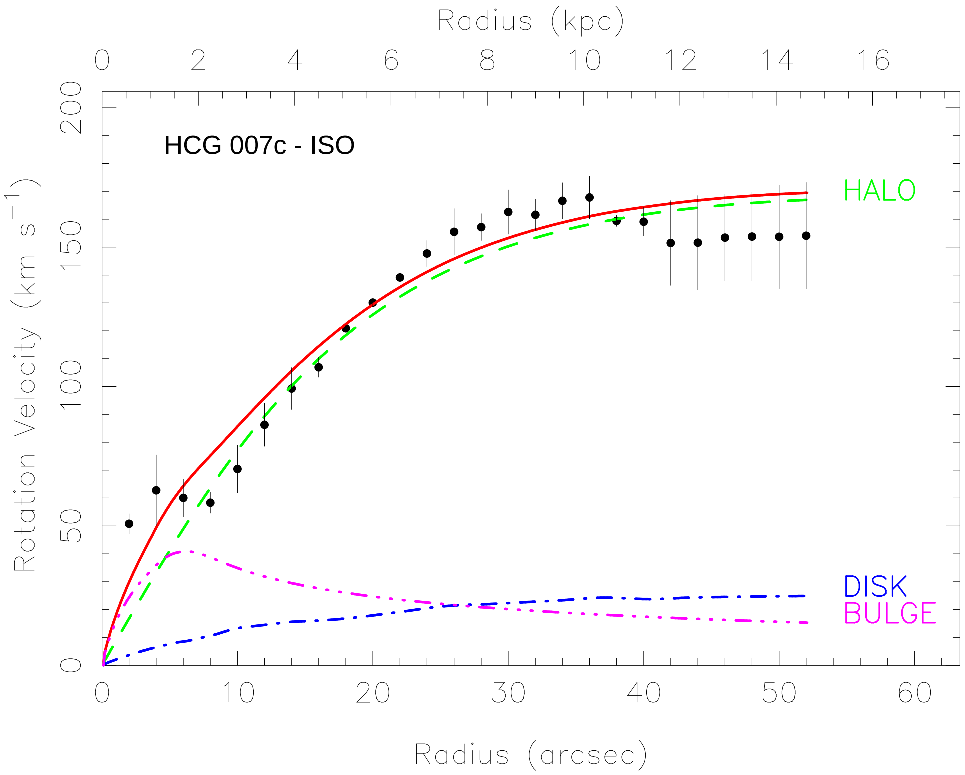

FIG. 4.— From figure 4 to 21, we present for each galaxy the J-band surface brightness (top) and the rotation curve (bottom). Disk and bulge components are represented together with the surface brightness and the fit result. Disk component is in blue and bulge is in red on the surface brightness profile. Disk, bulge and halo velocities components are represented together with the rotation curve

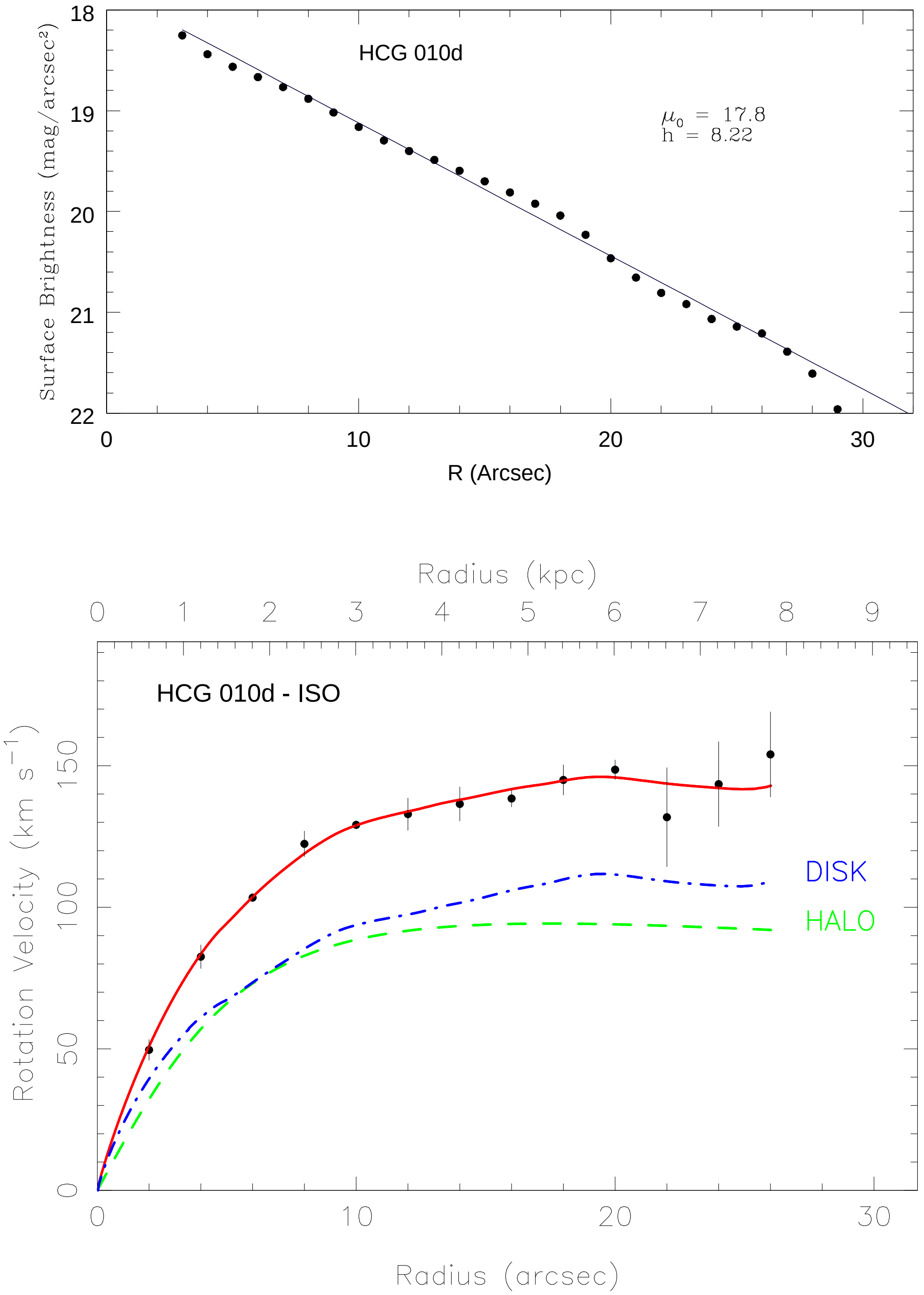
HCG 010d
μ_0 = 17.8
h = 8.22
Surface Brightness (mag/arcsec²)
18
19
20
21
22
0
10
20
30
R (Arcsec)
Radius (kpc)
0
1
2
3
4
5
6
7
8
9
HCG 010d - ISO
Rotation Velocity (km s⁻¹)
0
50
100
150
DISK
HALO
0
10
20
30
Radius (arcsec)

Fig. 5.—

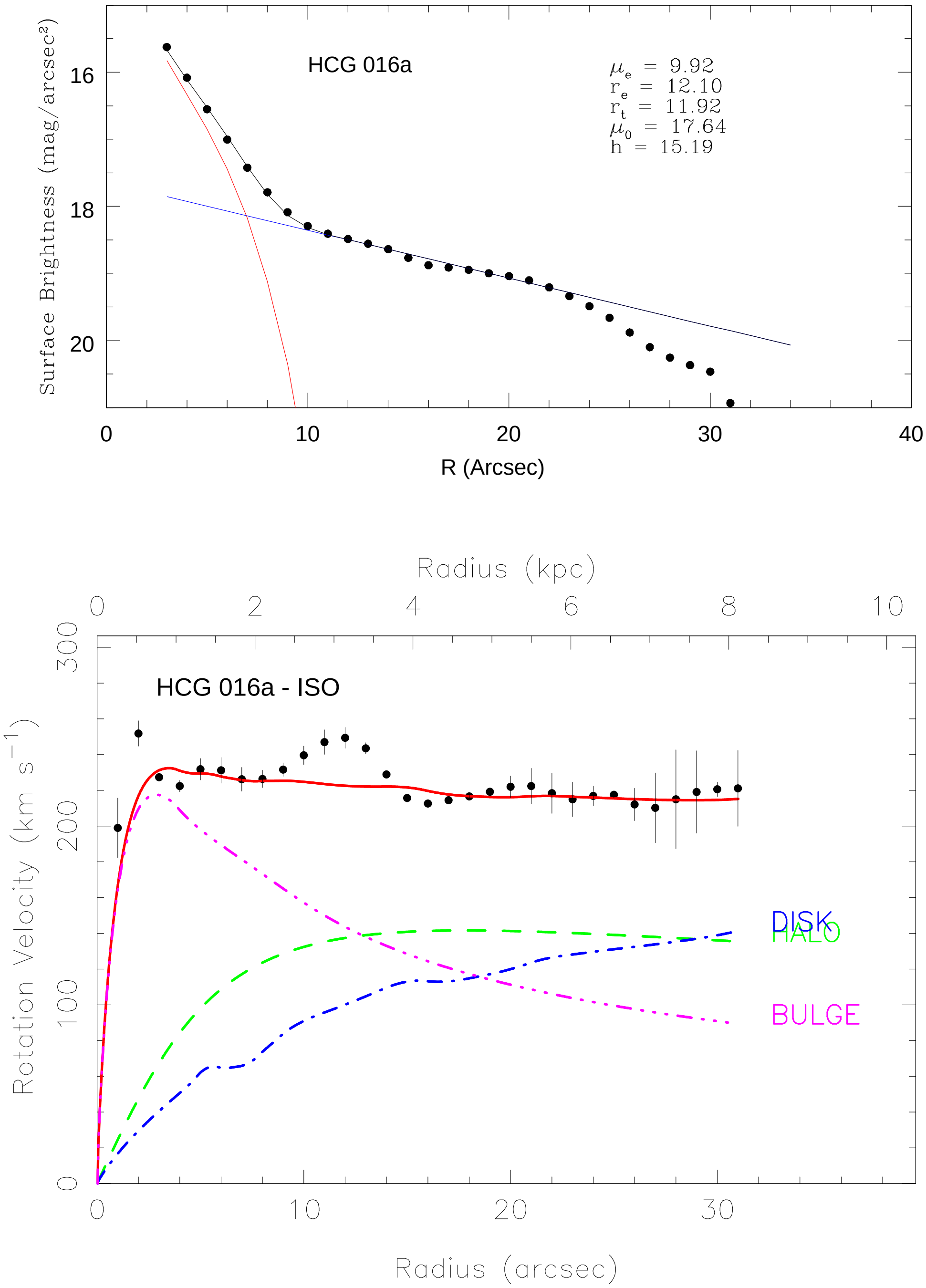
HCG 016a
μ_e = 9.92
r_e = 12.10
r_t = 11.92
μ_0 = 17.64
h = 15.19
Surface Brightness (mag/arcsec²)
16
18
20
0
10
20
30
40
R (Arcsec)
Radius (kpc)
0
2
4
6
8
10
HCG 016a - ISO
Rotation Velocity (km s^{-1})
0
100
200
300
DISK
HALO
BULGE
0
10
20
30
Radius (arcsec)

FIG. 6.—

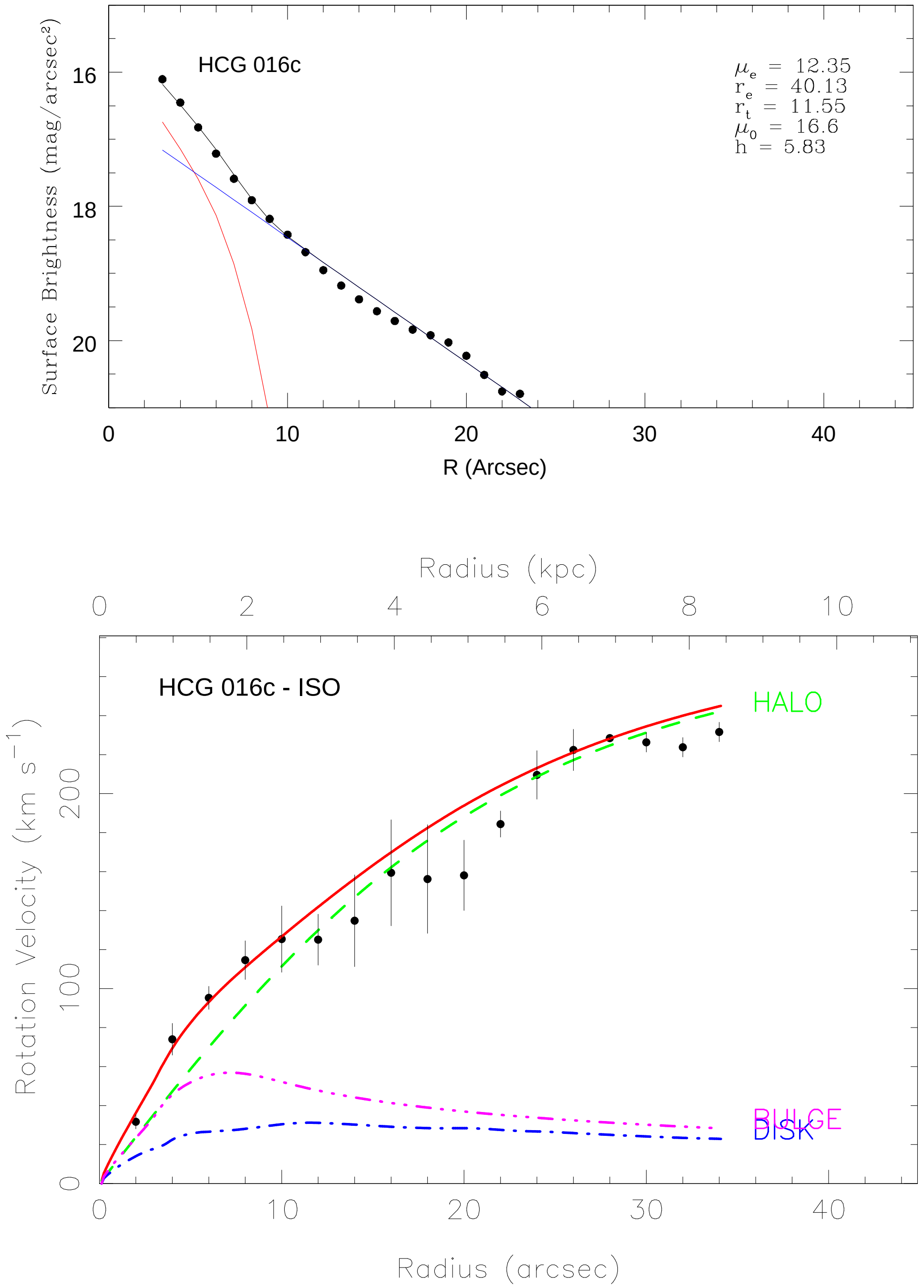
HCG 016c
μ_e = 12.35
r_e = 40.13
r_t = 11.55
μ_0 = 16.6
h = 5.83
Surface Brightness (mag/arcsec^2)
16
18
20
R (Arcsec)
0
10
20
30
40
Radius (kpc)
0
2
4
6
8
10
HCG 016c - ISO
HALO
BULGE
DISK
Rotation Velocity (km s^{-1})
0
100
200
0
10
20
30
40
Radius (arcsec)

FIG. 7.—

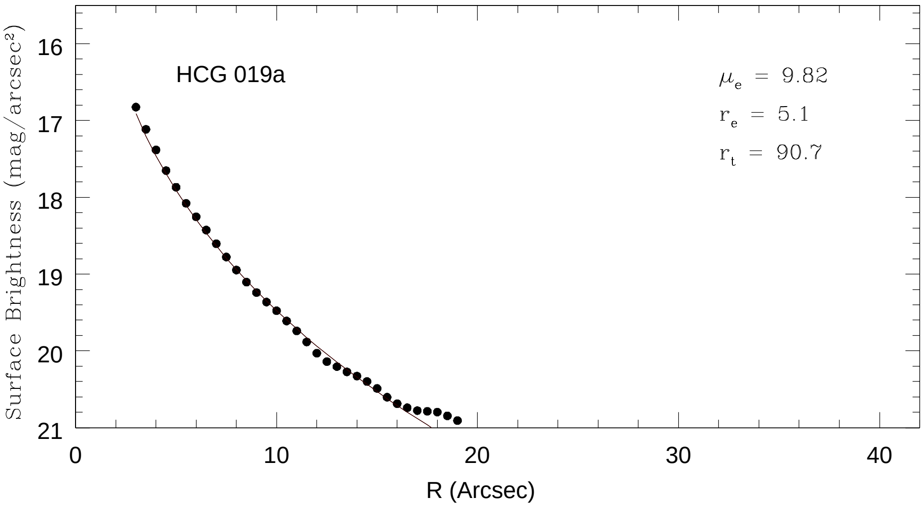
HCG 019a
μ_e = 9.82
r_e = 5.1
r_t = 90.7
Surface Brightness (mag/arcsec²)
16
17
18
19
20
21
0
10
20
30
40
R (Arcsec)

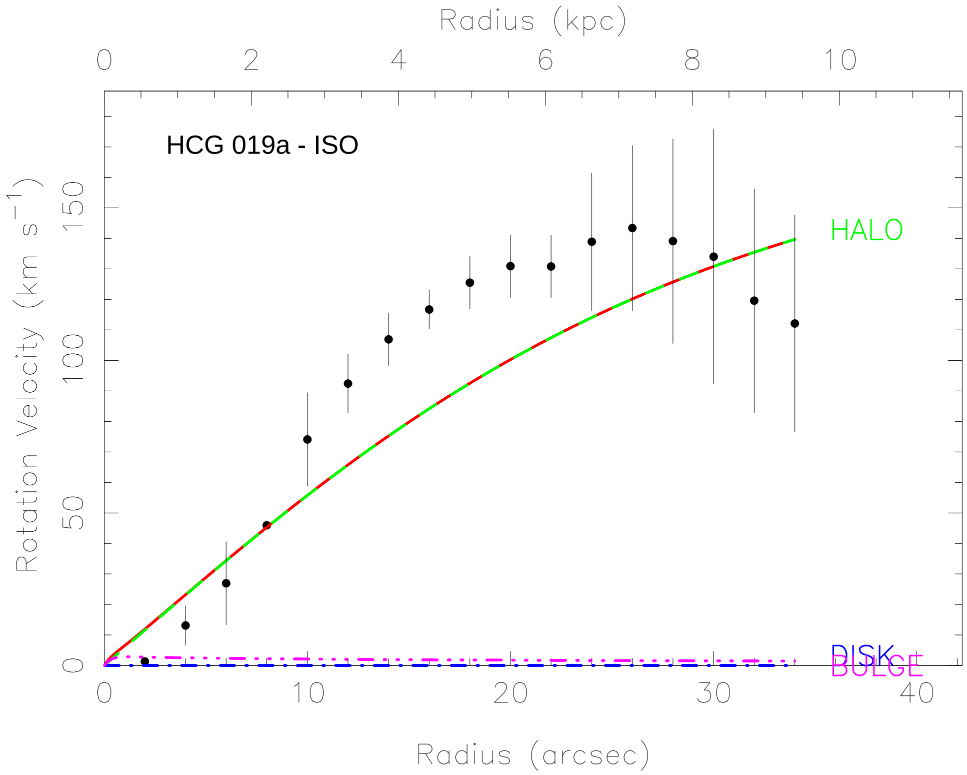
Radius (kpc)
0
2
4
6
8
10
HCG 019a - ISO
HALO
DISK
BULGE
Rotation Velocity (km s^{-1})
0
50
100
150
0
10
20
30
40
Radius (arcsec)

FIG. 8.—

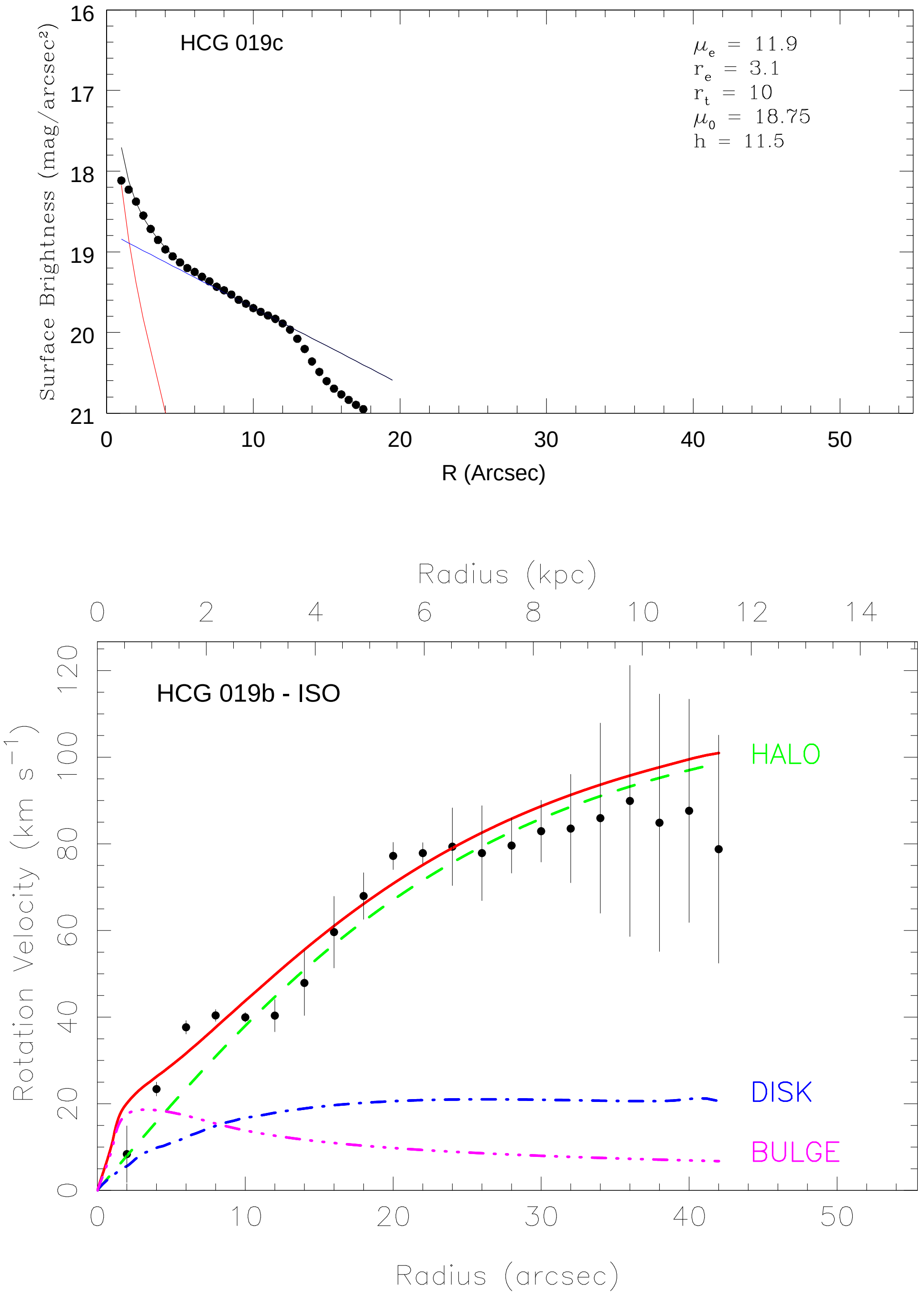
HCG 019c
μe = 11.9
re = 3.1
rt = 10
μ0 = 18.75
h = 11.5
Surface Brightness (mag/arcsec²)
16
17
18
19
20
21
0
10
20
30
40
50
R (Arcsec)
Radius (kpc)
0
2
4
6
8
10
12
14
HCG 019b - ISO
HALO
DISK
BULGE
Rotation Velocity (km s⁻¹)
0
20
40
60
80
100
120
0
10
20
30
40
50
Radius (arcsec)

Fig. 9.—

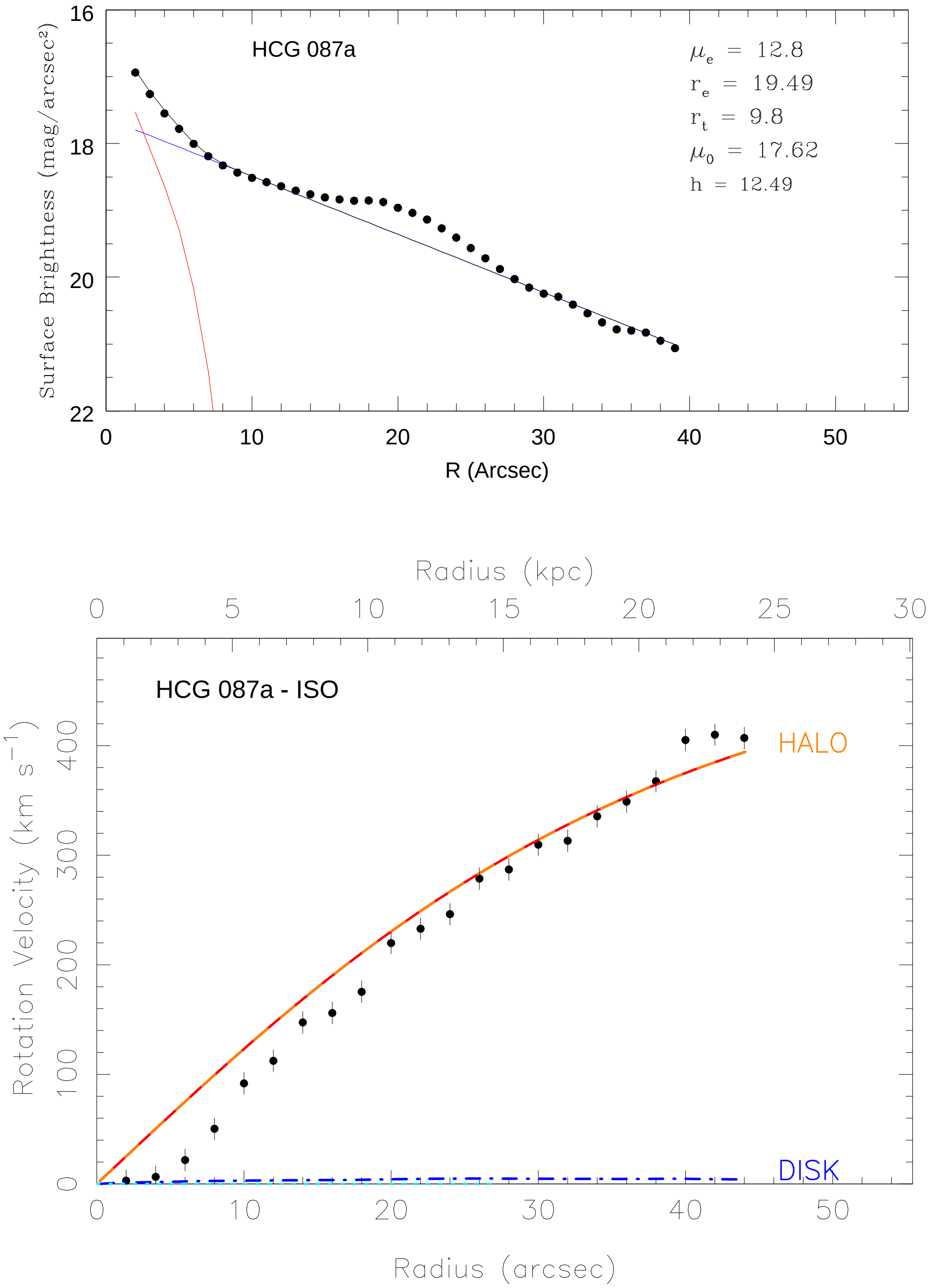
HCG 087a
μ_e = 12.8
r_e = 19.49
r_t = 9.8
μ_0 = 17.62
h = 12.49
Surface Brightness (mag/arcsec²)
16
18
20
22
0
10
20
30
40
50
R (Arcsec)
Radius (kpc)
0
5
10
15
20
25
30
HCG 087a - ISO
HALO
DISK
Rotation Velocity (km s^{-1})
0
100
200
300
400
0
10
20
30
40
50
Radius (arcsec)

Fig. 10.—

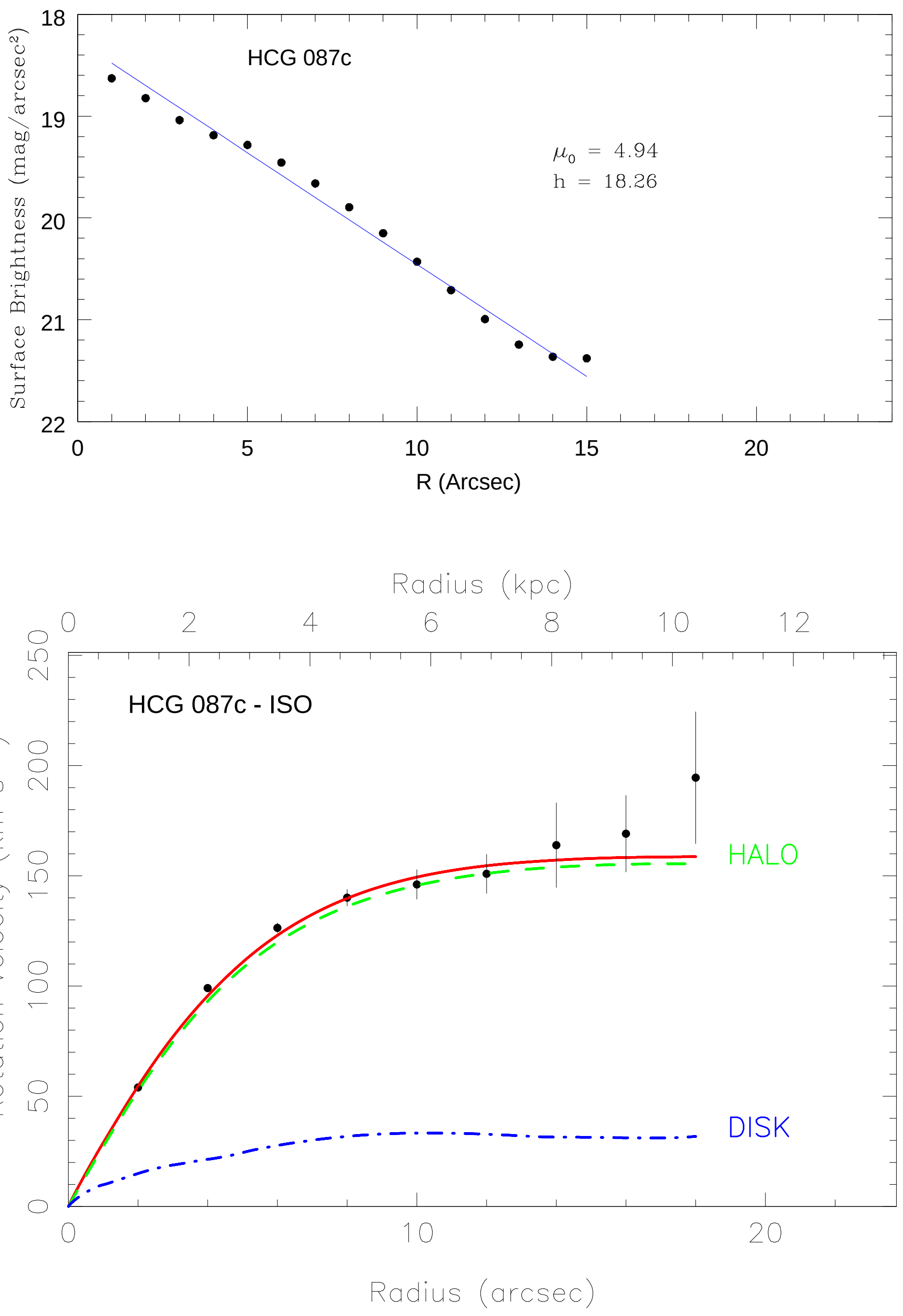
HCG 087c
μ_0 = 4.94
h = 18.26
Surface Brightness (mag/arcsec²)
18
19
20
21
22
0
5
10
15
20
R (Arcsec)
Radius (kpc)
0
2
4
6
8
10
12
HCG 087c - ISO
Rotation Velocity (km s^{-1})
0
50
100
150
200
250
HALO
DISK
0
10
20
Radius (arcsec)

Fig. 11.—

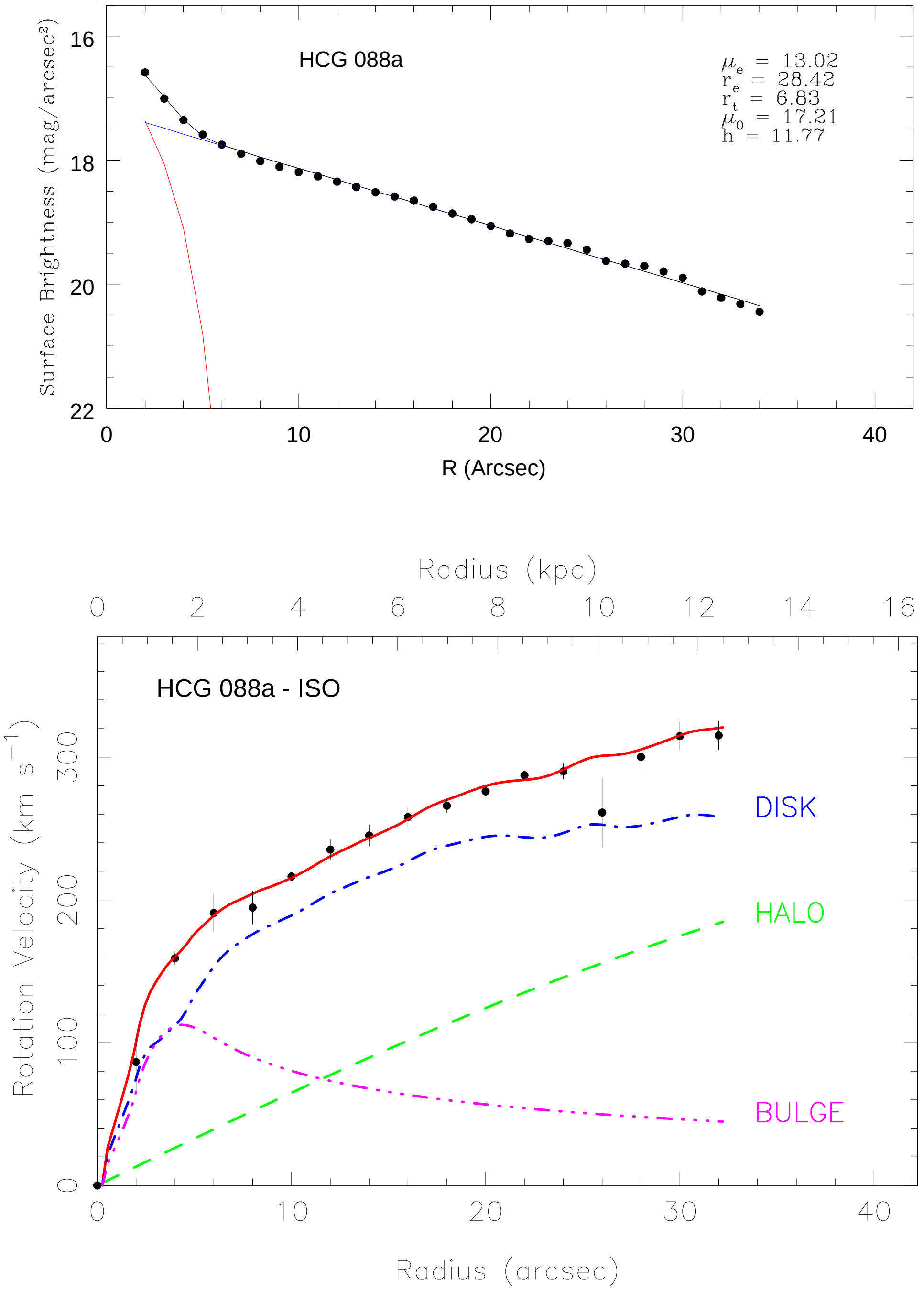
HCG 088a
μ_e = 13.02
r_e = 28.42
r_t = 6.83
μ_0 = 17.21
h = 11.77
Surface Brightness (mag/arcsec^2)
16
18
20
22
0
10
20
30
40
R (Arcsec)
Radius (kpc)
0
2
4
6
8
10
12
14
16
HCG 088a - ISO
DISK
HALO
BULGE
Rotation Velocity (km s^{-1})
0
100
200
300
0
10
20
30
40
Radius (arcsec)

Fig. 12.—

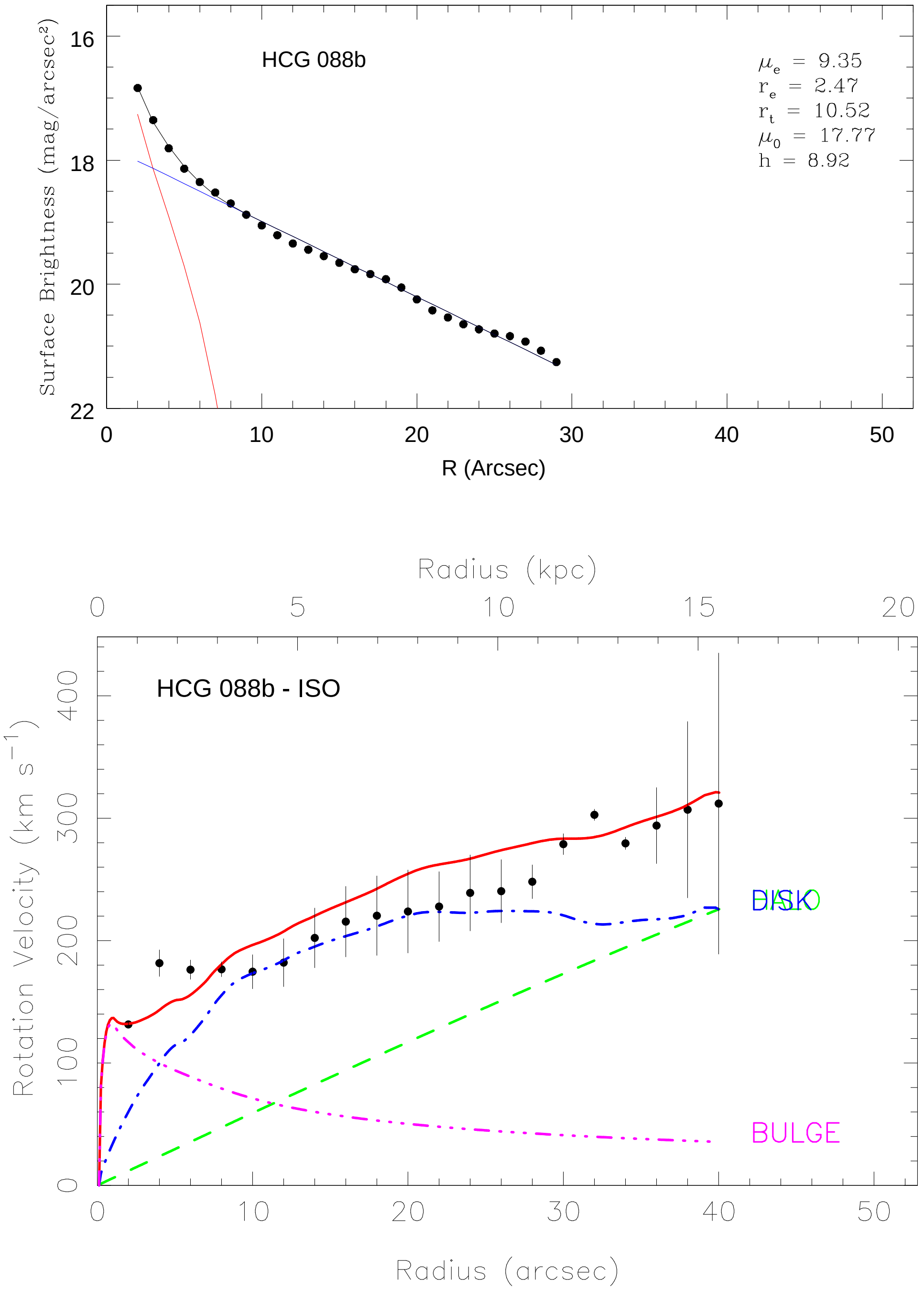
HCG 088b
μ_e = 9.35
r_e = 2.47
r_t = 10.52
μ_0 = 17.77
h = 8.92
Surface Brightness (mag/arcsec^2)
16
18
20
22
0
10
20
30
40
50
R (Arcsec)
Radius (kpc)
0
5
10
15
20
HCG 088b - ISO
Rotation Velocity (km s^{-1})
0
100
200
300
400
DISK
HALO
BULGE
0
10
20
30
40
50
Radius (arcsec)

Fig. 13.—

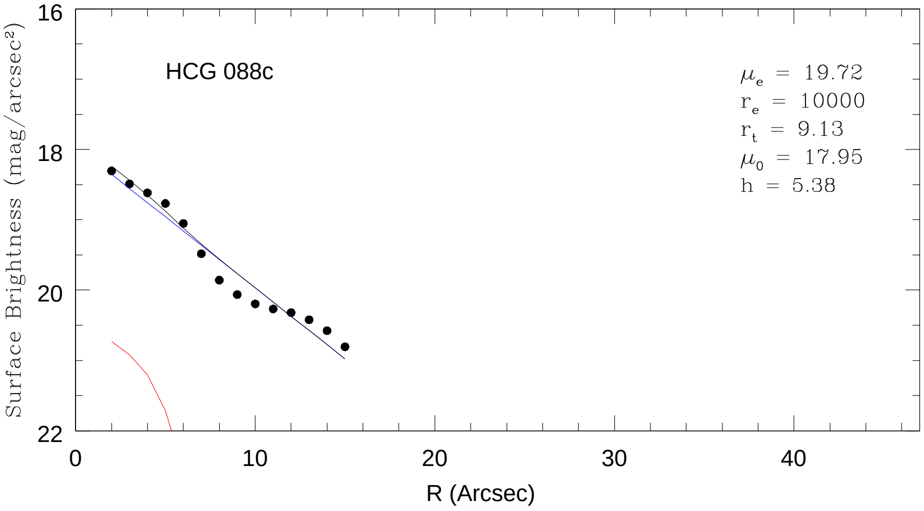
HCG 088c
μ_e = 19.72
r_e = 10000
r_t = 9.13
μ_0 = 17.95
h = 5.38
Surface Brightness (mag/arcsec^2)
16
18
20
22
0
10
20
30
40
R (Arcsec)

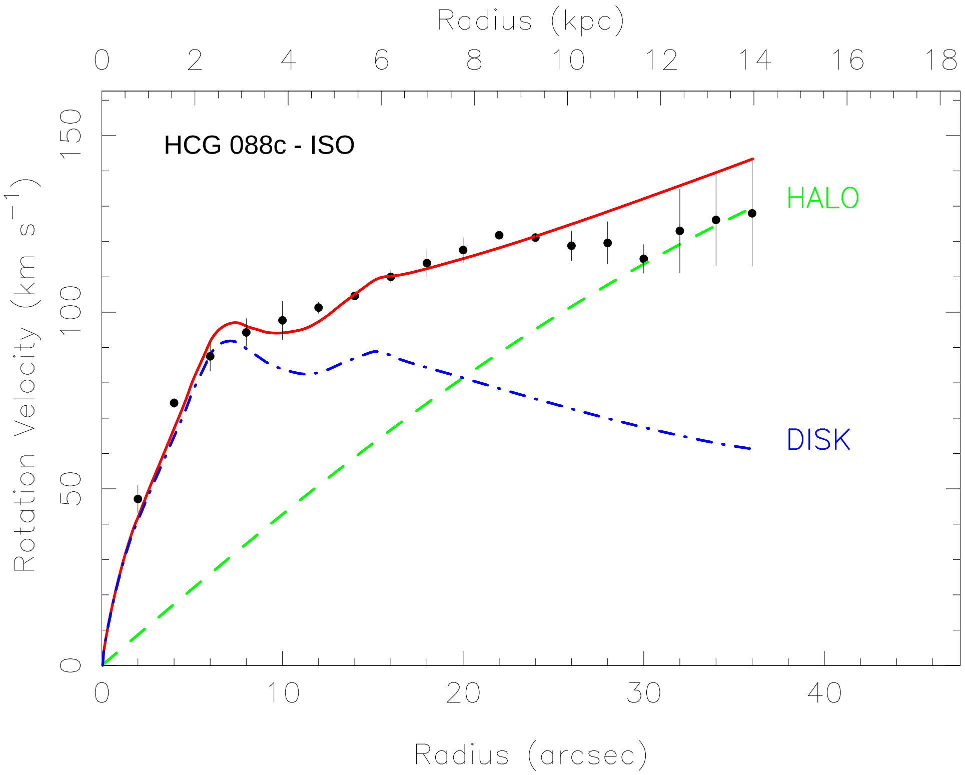
Radius (kpc)
0
2
4
6
8
10
12
14
16
18
HCG 088c - ISO
HALO
DISK
Rotation Velocity (km s^{-1})
0
50
100
150
0
10
20
30
40
Radius (arcsec)

FIG. 14.—

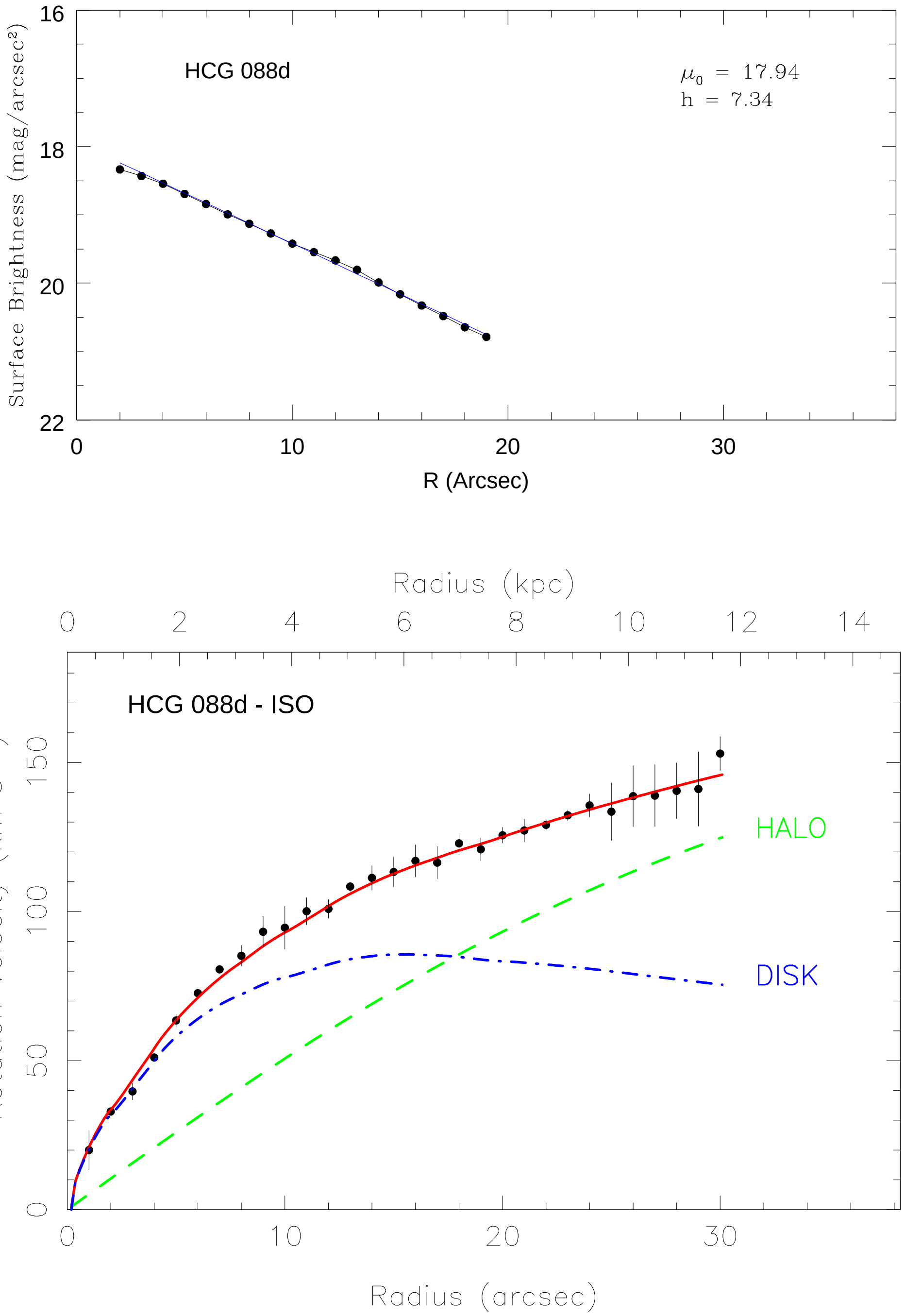
HCG 088d
μ_0 = 17.94
h = 7.34
Surface Brightness (mag/arcsec^2)
16
18
20
22
0
10
20
30
R (Arcsec)
Radius (kpc)
0
2
4
6
8
10
12
14
HCG 088d - ISO
Rotation Velocity (km s^{-1})
0
50
100
150
HALO
DISK
0
10
20
30
Radius (arcsec)

FIG. 15.—

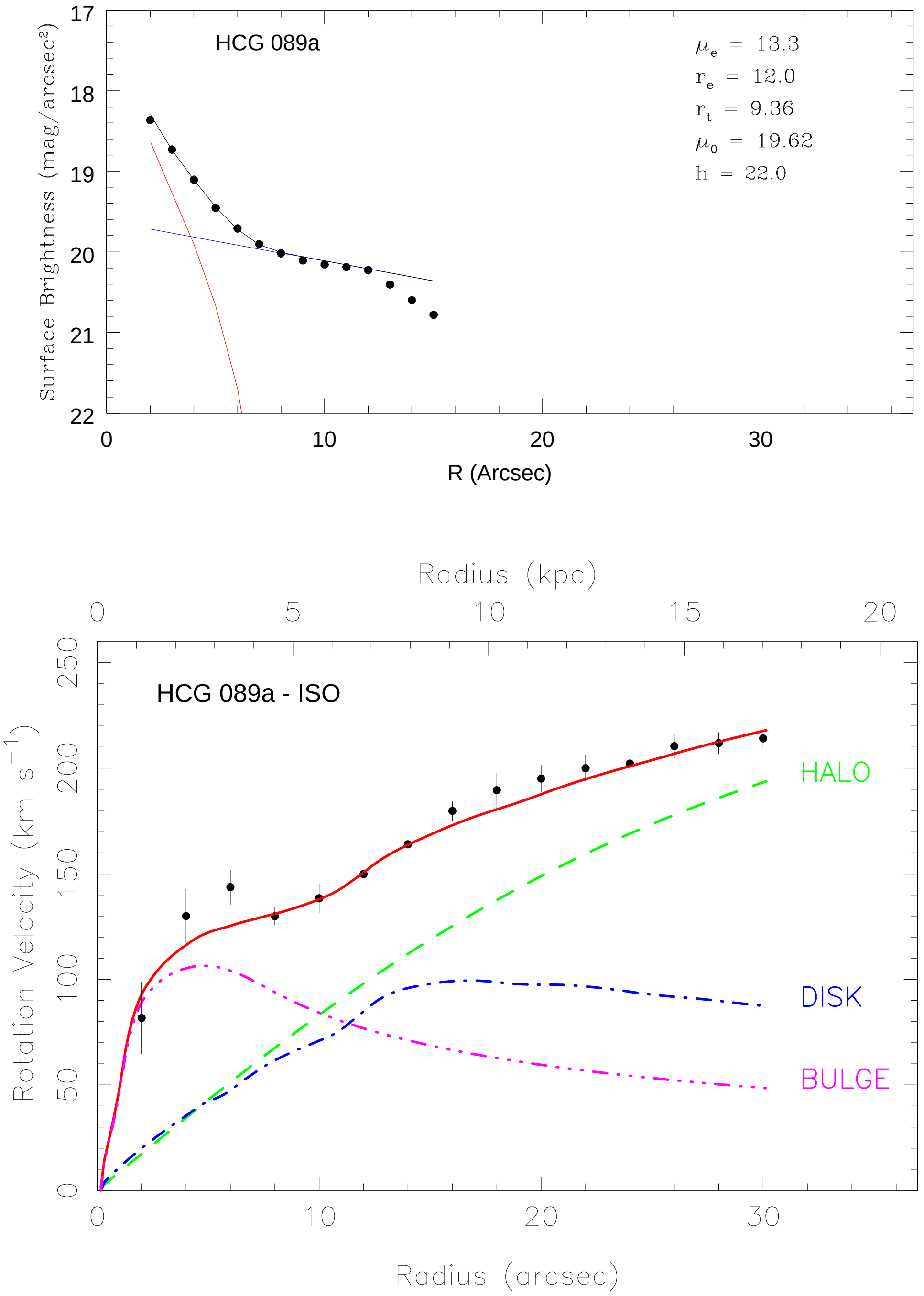
HCG 089a
μ_e = 13.3
r_e = 12.0
r_t = 9.36
μ_0 = 19.62
h = 22.0
Surface Brightness (mag/arcsec^2)
17
18
19
20
21
22
0
10
20
30
R (Arcsec)
Radius (kpc)
0
5
10
15
20
HCG 089a - ISO
Rotation Velocity (km s^{-1})
0
50
100
150
200
250
HALO
DISK
BULGE
Radius (arcsec)

FIG. 16.—

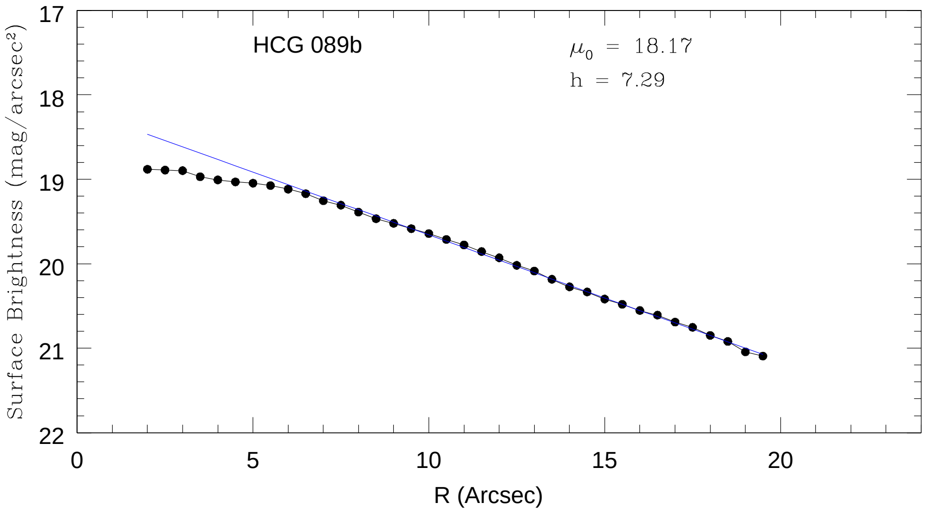
HCG 089b
μ_0 = 18.17
h = 7.29
Surface Brightness (mag/arcsec^2)
17
18
19
20
21
22
0
5
10
15
20
R (Arcsec)

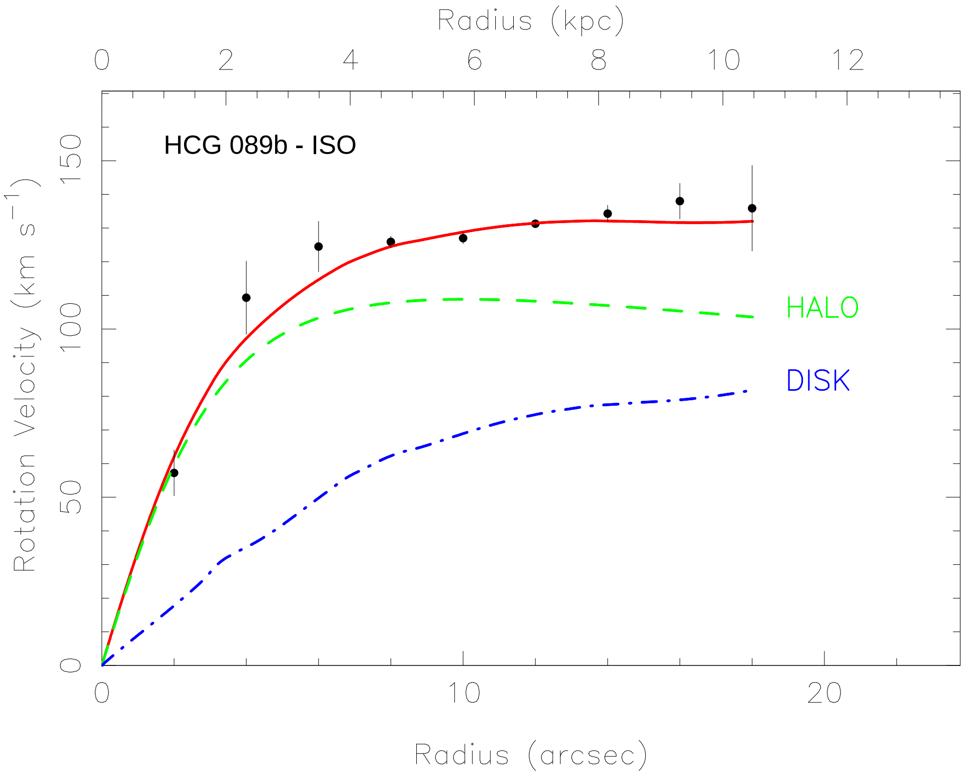
Radius (kpc)
0
2
4
6
8
10
12
HCG 089b - ISO
HALO
DISK
Rotation Velocity (km s^{-1})
0
50
100
150
0
10
20
Radius (arcsec)

FIG. 17.—

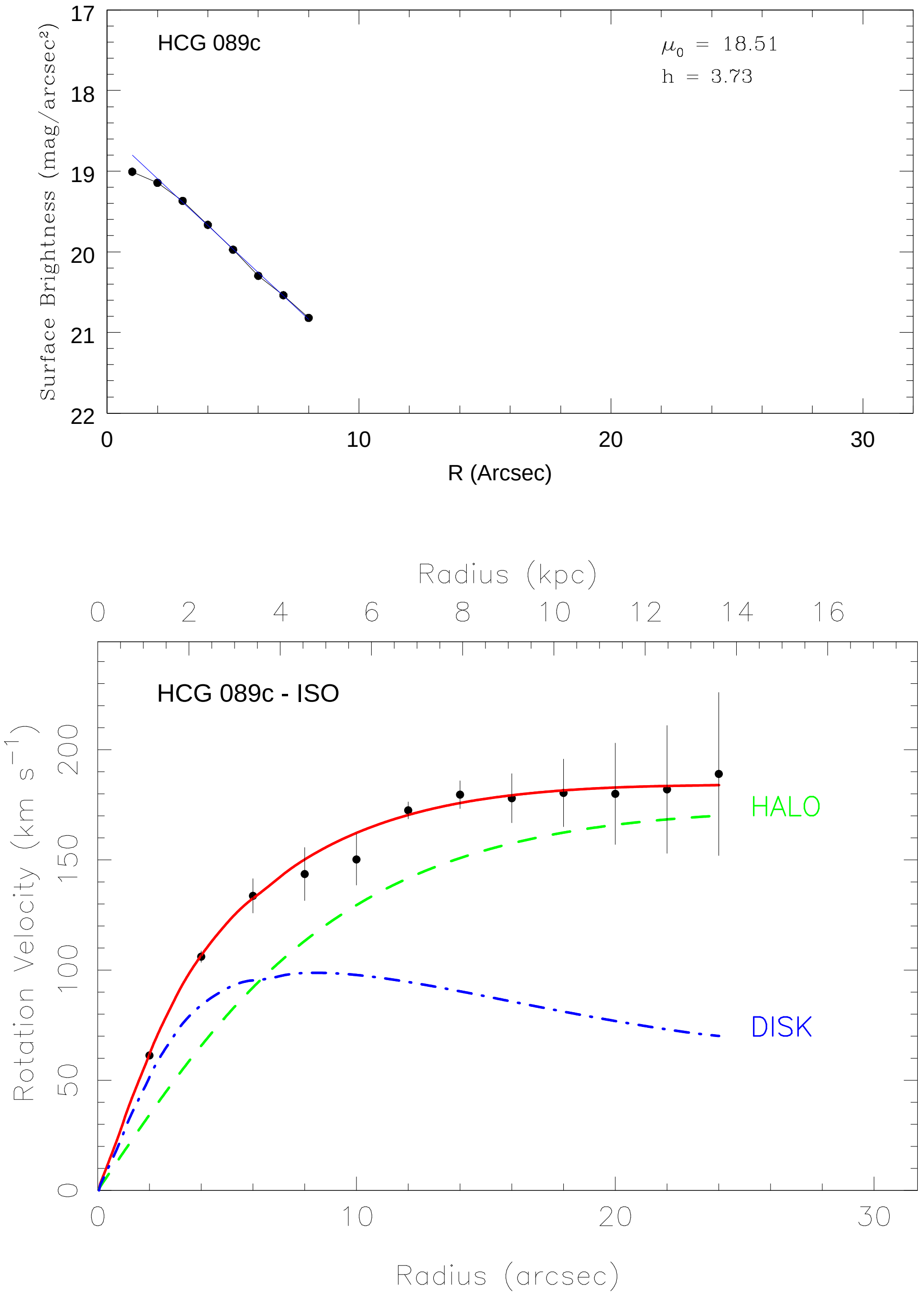
HCG 089c
μ_0 = 18.51
h = 3.73
Surface Brightness (mag/arcsec^2)
17
18
19
20
21
22
0
10
20
30
R (Arcsec)
Radius (kpc)
0
2
4
6
8
10
12
14
16
HCG 089c - ISO
Rotation Velocity (km s^{-1})
0
50
100
150
200
HALO
DISK
0
10
20
30
Radius (arcsec)

FIG. 18.—

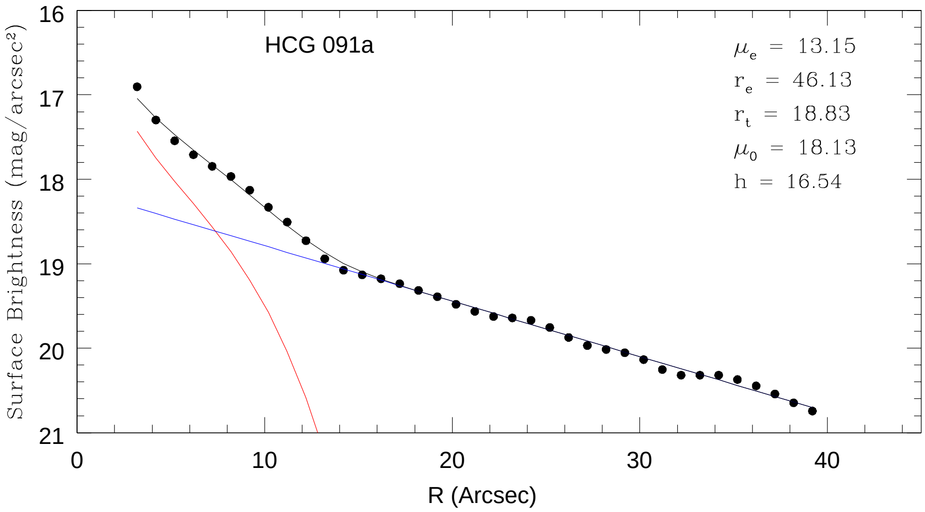
HCG 091a
μ_e = 13.15
r_e = 46.13
r_t = 18.83
μ_0 = 18.13
h = 16.54
Surface Brightness (mag/arcsec^2)
16
17
18
19
20
21
0
10
20
30
40
R (Arcsec)

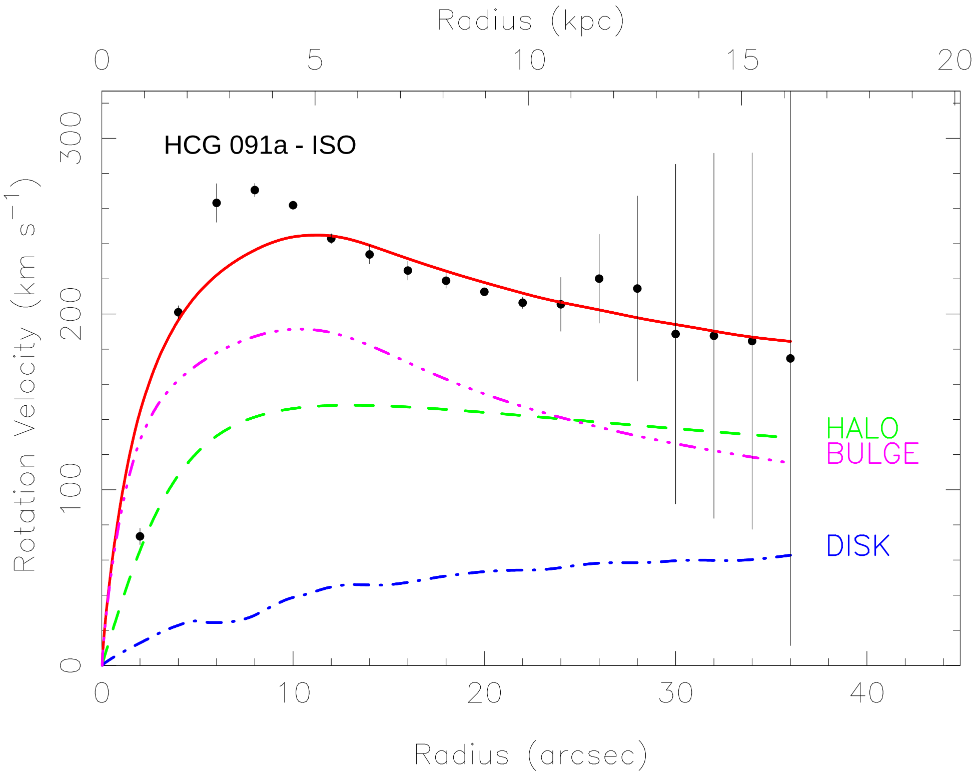
Radius (kpc)
0
5
10
15
20
HCG 091a - ISO
Rotation Velocity (km s^{-1})
0
100
200
300
HALO
BULGE
DISK
0
10
20
30
40
Radius (arcsec)

FIG. 19.—

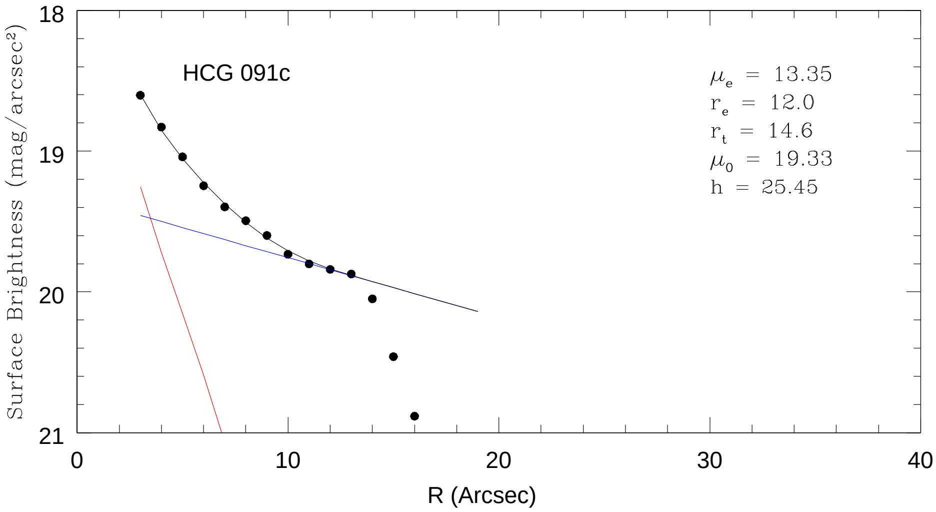
HCG 091c
μ_e = 13.35
r_e = 12.0
r_t = 14.6
μ_0 = 19.33
h = 25.45
Surface Brightness (mag/arcsec^2)
18
19
20
21
0
10
20
30
40
R (Arcsec)

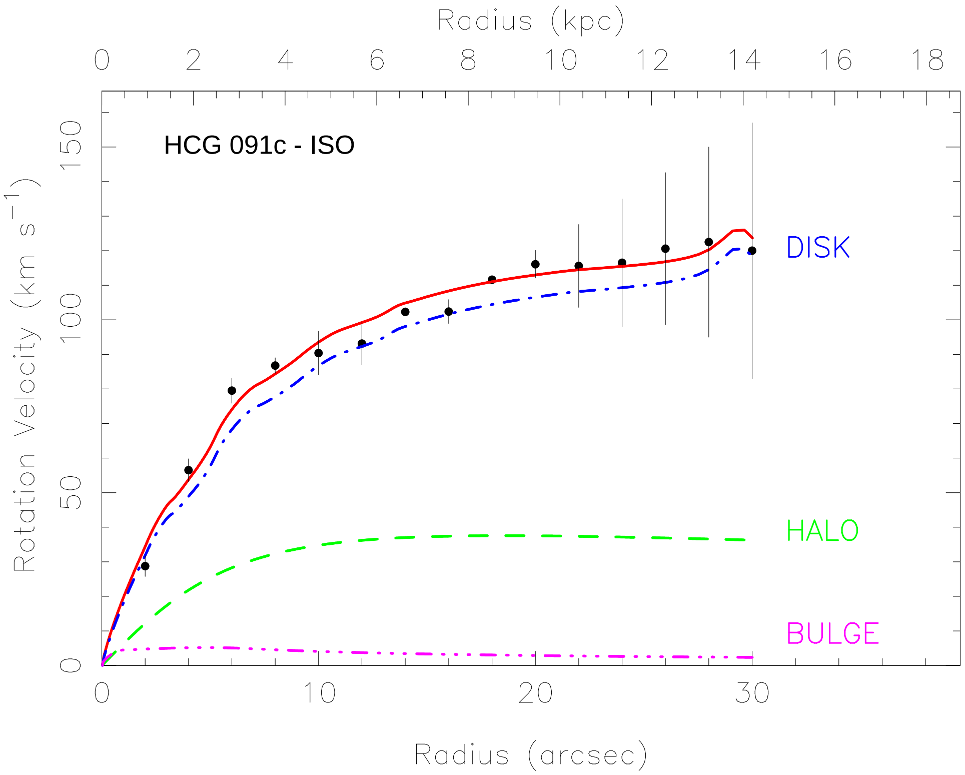
Radius (kpc)
0
2
4
6
8
10
12
14
16
18
HCG 091c - ISO
DISK
HALO
BULGE
Rotation Velocity (km s^{-1})
0
50
100
150
0
10
20
30
Radius (arcsec)

Fig. 20.—

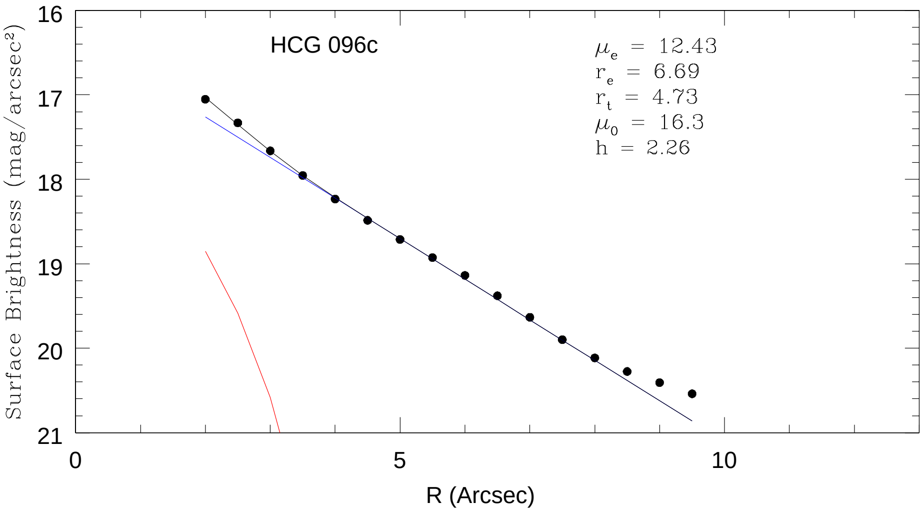
HCG 096c
μ_e = 12.43
r_e = 6.69
r_t = 4.73
μ_0 = 16.3
h = 2.26
Surface Brightness (mag/arcsec^2)
16
17
18
19
20
21
0
5
10
R (Arcsec)

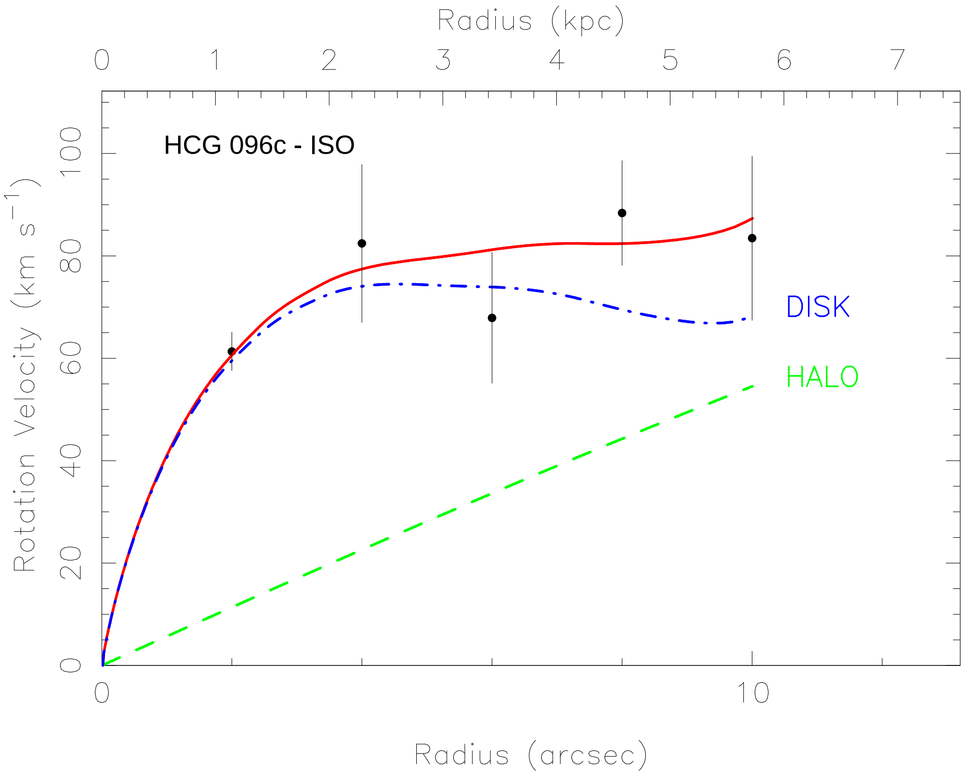
Radius (kpc)
0
1
2
3
4
5
6
7
HCG 096c - ISO
DISK
HALO
Rotation Velocity (km s^{-1})
0
20
40
60
80
100
0
10
Radius (arcsec)

FIG. 21.—

TABLE B1

Photometric and Mass Model parameters for the HCG with the isothermal sphere as the halo J-band

Name	Photometric Parameters						Mass Model Parameters				
HCG[1]	Inclination	${\mu_0}^2$	h^3	${\mu_e}^4$	${r_e}^5$	${r_t}^6$	${M/L_{bulge}}^7$	${M/L_{disk}}^8$	${r_0}^9$	${\rho_0}^{10}$	${\chi^2}_{11}$
h007c	48 ± 5	19.12	7.21	14.70	9.02	2.81	$0.55^{0.46}_{0.44}$	$0.05^{1.49}_{1.41}$	$6.00^{5.12}_{4.88}$	$0.05^{0.03}_{0.02}$	4.29
h010d	68 ± 5	17.80	2.47	0.00	0.00	0.00	$1.00^{1.02}_{0.98}$	$1.60^{1.95}_{1.85}$	$1.80^{1.74}_{1.66}$	$0.18^{0.15}_{0.15}$	0.39
h016a	43 ± 5	17.64	3.98	9.91	3.17	3.12	$0.20^{0.20}_{0.20}$	$0.40^{0.77}_{0.73}$	$1.60^{1.13}_{1.07}$	$0.50^{0.46}_{0.44}$	7.61
h016c	60 ± 5	16.60	1.44	12.35	9.92	2.86	$0.11^{0.05}_{0.05}$	$0.03^{0.10}_{0.10}$	$6.00^{5.12}_{4.88}$	$0.13^{0.16}_{0.16}$	3.00
h019a	53 ± 10	0.00	1.00	9.95	1.88	25.06	$0.00^{0.00}_{0.00}$	$0.10^{0.10}_{0.10}$	$9.00^{9.22}_{8.78}$	$0.02^{0.03}_{0.03}$	39.53
h019b	60 ± 10	18.75	3.12	11.90	0.84	2.71	$0.14^{0.03}_{0.02}$	$0.05^{0.22}_{0.20}$	$8.00^{18.45}_{17.55}$	$0.01^{0.01}_{0.01}$	3.13
h087a	85 ± 10	17.62	6.78	12.80	10.58	5.32	$0.00^{0.00}_{0.00}$	$0.00^{0.40}_{0.38}$	$23.00^{5.12}_{4.88}$	$0.03^{0.01}_{0.01}$	8.22
h087c	50 ± 3	18.26	2.85	0.00	0.00	0.00	$0.10^{0.10}_{0.10}$	$0.10^{0.20}_{0.20}$	$3.50^{4.10}_{3.90}$	$0.13^{0.11}_{0.11}$	2.07
h088a	65 ± 5	17.21	4.56	13.01	11.02	2.65	$1.05^{1.08}_{1.02}$	$1.75^{1.79}_{1.71}$	$21.00^{36.90}_{35.10}$	$0.02^{0.01}_{0.01}$	0.90
h088b	55 ± 3	18.13	4.56	9.10	1.12	4.27	$0.20^{0.20}_{0.20}$	$1.50^{1.84}_{1.75}$	$45.00^{77.90}_{74.10}$	$0.01^{0.01}_{0.01}$	3.64
h088c	42 ± 2	17.95	2.09	19.72	3882.00	3.54	$0.30^{0.31}_{0.29}$	$0.45^{0.50}_{0.48}$	$19.50^{24.09}_{22.91}$	$0.01^{0.01}_{0.01}$	5.89
h088d	70 ± 2	17.94	2.85	0.00	0.00	0.00	$0.10^{0.10}_{0.10}$	$0.97^{1.02}_{0.98}$	$14.50^{14.86}_{14.14}$	$0.01^{0.01}_{0.01}$	1.20
h089a	45 ± 5	19.62	12.48	13.30	6.81	5.31	$1.20^{1.13}_{1.07}$	$0.80^{0.92}_{0.88}$	$18.00^{20.50}_{19.50}$	$0.01^{0.01}_{0.01}$	1.28
h089b	49 ± 3	18.17	4.24	0.00	0.00	0.00	$1.00^{1.02}_{0.98}$	$0.70^{1.02}_{0.98}$	$2.00^{1.54}_{1.46}$	$0.19^{0.29}_{0.28}$	1.28
h089c	46 ± 3	18.51	2.12	0.00	0.00	0.00	$1.00^{1.02}_{0.98}$	$1.10^{1.23}_{1.17}$	$6.00^{8.20}_{7.80}$	$0.05^{0.04}_{0.04}$	0.28
h091a	50 ± 3	18.13	7.42	13.15	20.69	8.44	$1.00^{1.02}_{0.98}$	$0.10^{0.20}_{0.20}$	$2.00^{2.05}_{1.95}$	$0.35^{0.33}_{0.31}$	33.14
h091c	40 ± 5	18.76	5.08	14.80	12.78	4.26	$0.00^{0.01}_{0.01}$	$0.70^{0.80}_{0.76}$	$3.00^{2.05}_{1.95}$	$0.01^{0.01}_{0.01}$	1.66
h096c	57 ± 5	16.30	1.29	12.43	3.83	2.50	$0.05^{0.05}_{0.05}$	$0.16^{0.16}_{0.16}$	$18.00^{36.90}_{35.10}$	$0.01^{0.01}_{0.01}$	0.81

Note. — [1] Hickson Group, [2] Inclination of the disk from velocity fields, [3] Disk central surface brightness in $mag/arcsec^2$, [4] Scale length in kpc, [5] Bulge central surface brightness in $mag/arcsec^2$, [6] Characteristic radius in kpc, [7] Generalized characteristic radius kpc, [8] Mass / Luminosity ratio for the bulge in $M_\odot/L_\odot$, [9] Mass / Luminosity ratio for the disk in $M_\odot/L_\odot$, [10] Characteristic radius for the Dark Halo in kpc, [11] Central density for the dark halo in $M_\odot$ pc^{-3}, [12] Reduced χ^2

TABLE B2

HALO AND M/L PARAMETERS FOR THE HCG WITH MAXIMUM DISK AND NFW MODELS

Name	Halo & M/L Parameters MDM Model					Halo & M/L Parameters NFW Model				
HCG[1]	$M/L_{bulge}{}^{2}$	$M/L_{disk}{}^{3}$	$r_0{}^{4}$	$\rho_0{}^{5}$	χ^2	$M/L_{bulge}{}^{6}$	$M/L_{disk}{}^{7}$	$r_0{}^{8}$	$\rho_0{}^{9}$	$\chi^2{}_{10}$
h007c	0.45	1.45	5.00	0.03	5.13	$0.00^{0.01}_{0.00}$	$1.95^{2.05}_{1.90}$	$6.00^{6.15}_{5.85}$	$0.01^{0.01}_{0.01}$	5.50
h010d	1.00	1.90	1.70	0.15	0.43	$1.00^{1.02}_{0.98}$	$2.70^{2.77}_{2.63}$	$2.50^{2.80}_{2.10}$	$0.03^{0.03}_{0.02}$	1.42
h016a	0.20	0.75	1.10	0.45	9.04	$0.15^{0.15}_{0.15}$	$0.35^{0.36}_{0.34}$	$1.70^{1.74}_{1.66}$	$0.75^{0.77}_{0.73}$	7.54
h016c	0.05	0.10	5.00	0.16	3.52	$0.00^{0.05}_{0.00}$	$0.01^{0.04}_{0.01}$	$35.00^{35.88}_{34.12}$	$0.01^{0.01}_{0.01}$	14.27
h019a	0.00	0.10	9.00	0.03	45.26	$0.00^{0.00}_{0.00}$	$0.10^{0.10}_{0.10}$	$12.00^{12.30}_{11.70}$	$0.00^{0.00}_{0.00}$	189.79
h019b	0.03	0.21	18.00	0.01	3.65	$0.00^{0.05}_{0.00}$	$0.00^{0.04}_{0.00}$	$32.00^{35.00}_{29.00}$	$0.00^{0.00}_{0.00}$	7.53
h087a	0.00	0.39	5.00	0.01	1.19	$0.00^{0.00}_{0.00}$	$0.01^{0.15}_{0.01}$	$54.00^{55.00}_{52.00}$	$0.01^{0.01}_{0.01}$	59.36
h087c	0.10	0.20	4.00	0.11	2.47	$0.10^{0.10}_{0.10}$	$1.40^{1.43}_{1.37}$	$1.00^{1.02}_{0.98}$	$0.01^{0.01}_{0.01}$	63.94
h088a	1.05	1.75	36.00	0.01	1.03	$0.80^{1.05}_{0.55}$	$1.00^{1.02}_{0.98}$	$130.00^{133.25}_{126.75}$	$0.00^{0.00}_{0.00}$	0.72
h088b	0.20	1.80	76.00	0.01	4.33	$0.10^{0.10}_{0.10}$	$0.50^{0.70}_{0.49}$	$16.00^{16.40}_{15.60}$	$0.03^{0.03}_{0.02}$	4.54
h088c	0.30	0.49	23.50	0.01	6.91	$0.30^{0.31}_{0.29}$	$0.03^{0.04}_{0.01}$	$13.00^{13.32}_{12.68}$	$0.01^{0.01}_{0.01}$	5.33
h088d	0.10	1.00	14.50	0.01	1.44	$0.10^{0.10}_{0.10}$	$1.39^{1.45}_{1.34}$	$19.95^{20.45}_{17.95}$	$0.00^{0.00}_{0.00}$	61.71
h089a	1.10	0.90	20.00	0.01	1.43	$0.15^{0.25}_{0.00}$	$0.11^{0.15}_{0.07}$	$67.00^{68.67}_{65.33}$	$0.00^{0.00}_{0.00}$	3.76
h089b	1.00	1.00	1.50	0.28	1.51	$1.00^{1.02}_{0.98}$	$0.80^{0.82}_{0.78}$	$3.00^{3.07}_{2.93}$	$0.10^{0.11}_{0.10}$	3.22
h089c	1.00	1.20	8.00	0.04	0.33	$1.00^{1.02}_{0.98}$	$0.01^{0.11}_{0.01}$	$97.00^{101.00}_{92.00}$	$0.00^{0.00}_{0.00}$	9.88
h091a	1.00	0.20	2.00	0.32	37.54	$1.60^{1.64}_{1.56}$	$0.01^{0.01}_{0.01}$	$10.00^{10.25}_{9.00}$	$0.01^{0.01}_{0.01}$	36.49
h091c	0.01	0.78	2.00	0.01	1.95	$0.00^{0.09}_{0.00}$	$0.79^{0.81}_{0.77}$	$1.00^{5.00}_{0.98}$	$0.00^{0.01}_{0.00}$	1.74
h096c	0.05	0.16	36.00	0.01	0.98	$0.05^{0.05}_{0.05}$	$0.11^{0.11}_{0.11}$	$9.00^{11.00}_{7.00}$	$0.01^{0.01}_{0.00}$	0.82

NOTE. — [1] Hickson Group, [2] Mass / Luminosity ratio for the disk in $M_\odot/L_\odot$ using MDM model, [3] Mass / Luminosity ratio for the bulge in $M_\odot/L_\odot$ using MDM model, [4] Characteristic radius for the Dark Halo in kpc using MDM model, [5] Central density for the dark halo in $M_\odot$ pc^{-3} using MDM model, [6] Mass / Luminosity ratio for the bulge in $M_\odot/L_\odot$ using NFW model, [7] Mass / Luminosity ratio for the disk in $M_\odot/L_\odot$ using NFW model, [8] Characteristic radius for the Dark Halo in kpc using NFW model, [9] Central density for the dark halo in $M_\odot$ pc^{-3} using NFW model, [10] Reduced χ^2

TABLE B3
Table summarising the coefficients of the linear regression: $\log(\rho_0) = Alog(r_0) - B$.

Coef/Corr	ISO Model			NFW Model			MDM Model
	HCG Galaxies	Field Galaxies	Cluster Galaxies	HCG Galaxies	Field Galaxies	Cluster Galaxies	
A	-1.0 ± 0.22	-1.03 ± 0.20	-1.62 ± 0.12	-0.53 ± 0.24	-1.15 ± 0.30	-1.72 ± 0.09	
B	-0.47 ± 0.21	-0.68 ± 0.67	-0.28 ± 0.05	-1.50 ± 0.3	-0.76 ± 0.20	-0.20 ± 0.12	
Corr	-0.80 ± 0.21	-0.83 ± 0.17	-0.92 ± 0.07	-0.48 ± 0.46	-0.48 ± 0.37	-0.98 ± 0.17	-0.70 ± 0.26

TABLE B4
Mass table for HCG in J-band for ISO, MDM and NFW models

		ISO Model			MDM Model			NFW Model		
HCG	Distance Mpc	Disk Mass 10^{10} $M_\odot$	Halo Mass 10^{10} $M_\odot$	M_{Halo} / M_{Total}	Disk Mass 10^{10} $M_\odot$	Halo Mass 10^{10} $M_\odot$	M_{Halo} / M_{Total}	Disk Mass 10^{10} $M_\odot$	Halo Mass 10^{10} $M_\odot$	M_{Halo} / M_{Total}
h007c	58.00	0.18	9.5	0.98	5.1	3.3	0.39	6.8	1.40	0.17
h010d	62.00	1.5	1.5	0.50	1.8	1.2	0.40	2.5	0.32	0.11
h016a	54.00	2.6	3.5	0.57	5.0	1.3	0.21	2.3	4.30	0.65
h016c	51.00	0.081	12.0	0.99	0.27	11.0	0.98	0.027	12.00	1.00
h019a	57.00	0.45	4.3	0.91	0.45	5.0	0.92	0.45	9.0	0.67
h019b	56.00	0.050	2.6	0.98	0.32	2.7	0.90	0.0	1.70	1.00
h087a	112.00	0.0	86	1.00	2.8	0.94	0.25	0.072	59.00	1.00
h087c	119.00	0.16	5.8	0.97	0.32	6.6	0.95	2.2	0.019	0.01
h088a	80.00	14.0	9.9	0.42	14.0	11.0	0.45	7.8	18.00	0.70
h088b	80.00	12.0	18.0	0.61	14.0	14.0	0.50	3.9	24.00	0.86
h088c	80.00	1.0	5.4	0.84	1.1	5.2	0.82	0.069	5.30	0.99
h088d	80.00	1.2	4.2	0.78	1.2	4.2	0.78	1.7	0.09	0.05
h089a	117.00	2.2	15.0	0.87	2.5	15.0	0.86	0.31	18.00	0.98
h089b	120.00	0.84	2.6	0.76	1.6	2.0	0.56	1.3	2.6	0.67
h089c	117.00	1.1	9.1	0.90	1.4	11.0	0.88	0.012	15.00	1.00
h091a	92.50	1.1	6.3	0.85	2.2	5.8	0.72	0.11	3.0	0.96
h091c	97.60	2.8	0.43	0.13	3.1	0.084	0.03	3.2	0.002	0.00
h096c	118.00	0.45	0.40	0.47	0.45	0.54	0.55	0.31	0.52	0.63

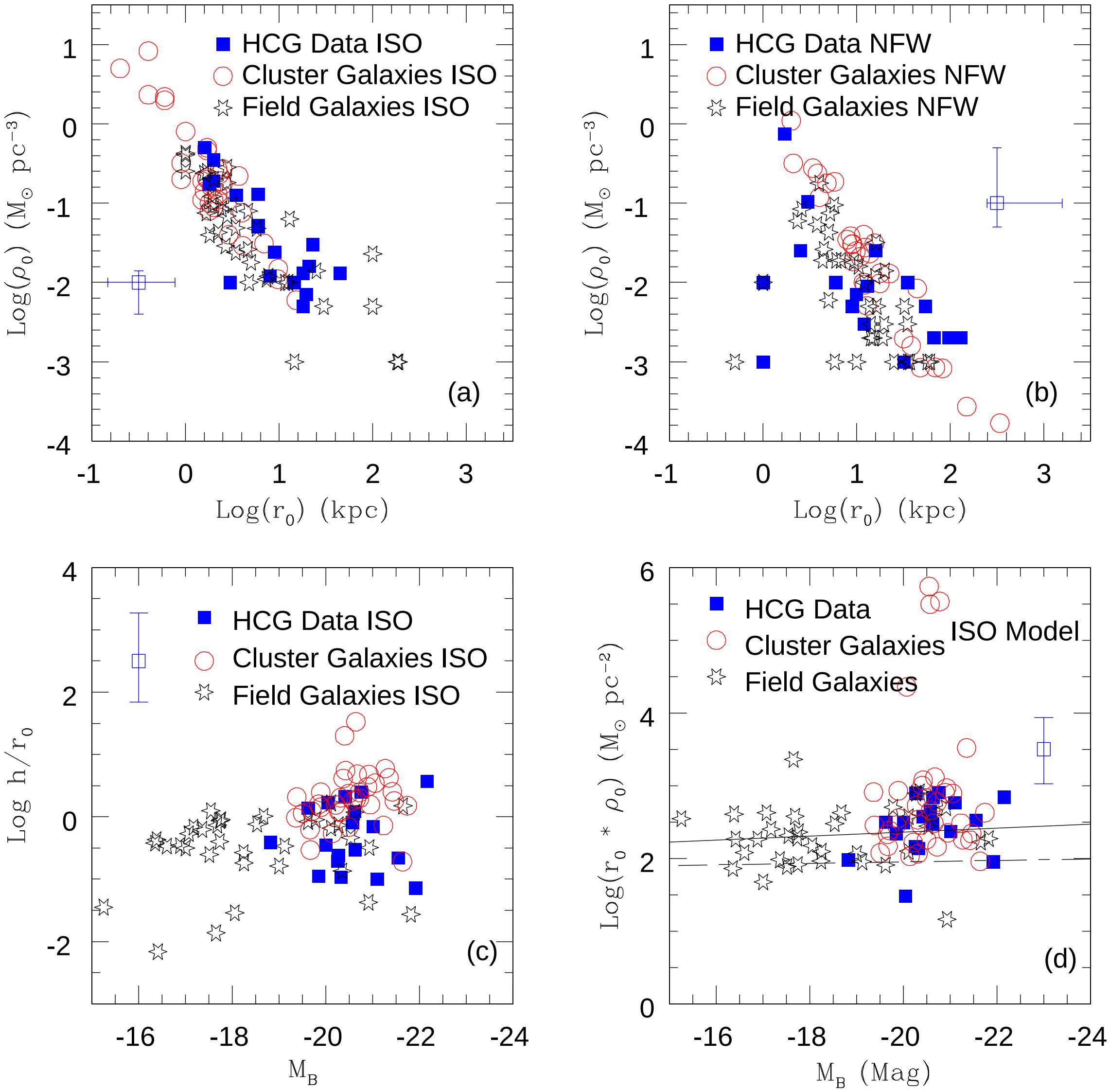

FIG. B1.— Fig. 1a,b: Correlation between the central halo density and the halo core radius using the ISO model (a) and the NFW (b). Fig. 1c: Relation between the disk scale length normalised to the core radius vs the B absolute magnitude. Fig. 1d represents the halo central surface density vs the B absolute magnitude. The line represents the linear regression of the field galaxies and the dashed line represents the linear regression shown by (Kormendy 2004). In each plot, error bars represent the maximum error found by the fit for each parameter.

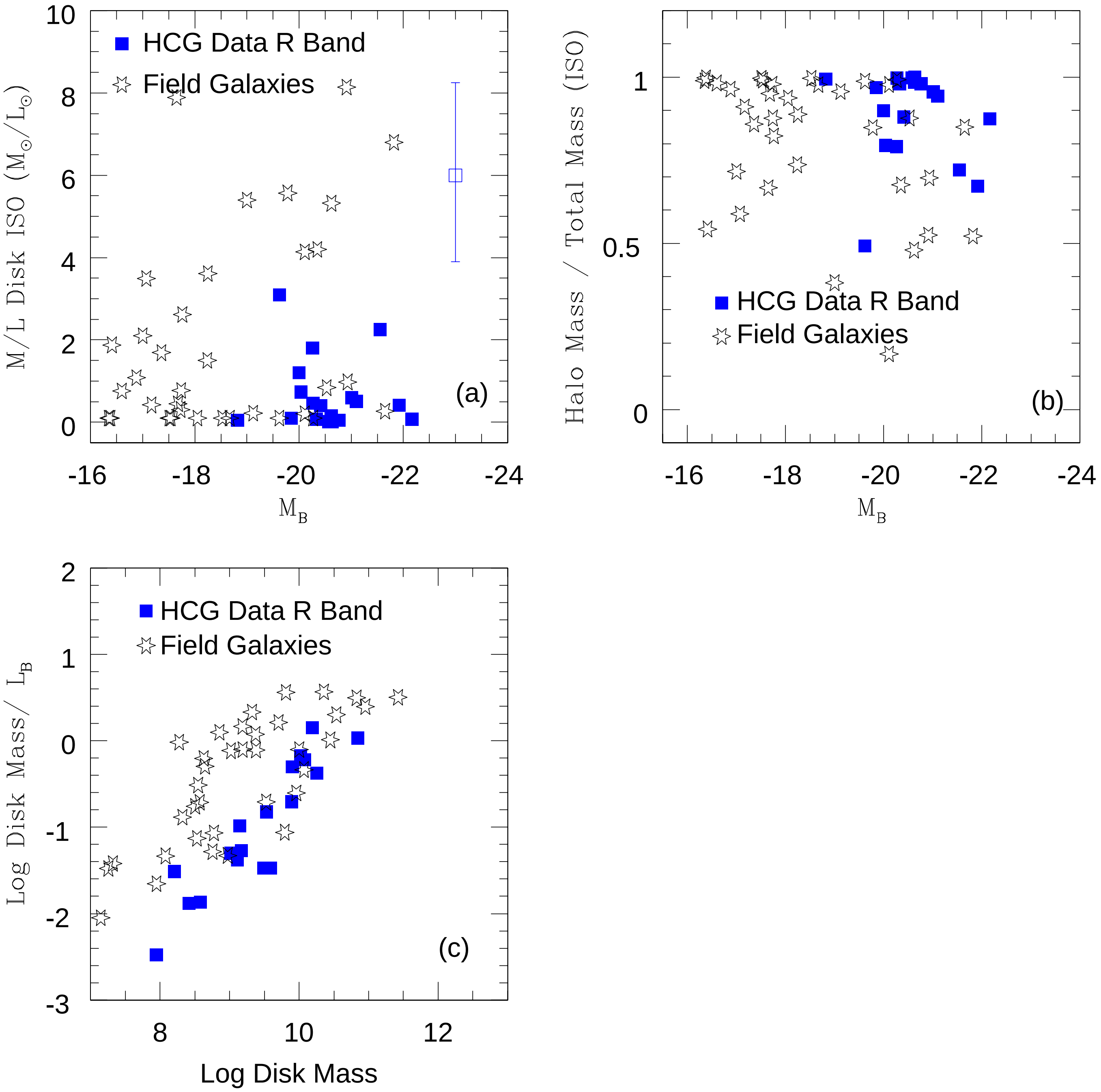

Fig. B2.— Fig 2a represents the disk M/L using the ISO model vs the absolute B magnitude for both field and HCG galaxies. In each plot, error bars represent the maximum error found by the fit for each parameter. Fig. 2b represents the halo mass fraction (normalised to the total mass) using ISO vs NFW for both field and HCG galaxies. Fig. 2c shows the disk mass divided by the total B luminosity vs the disk mass.

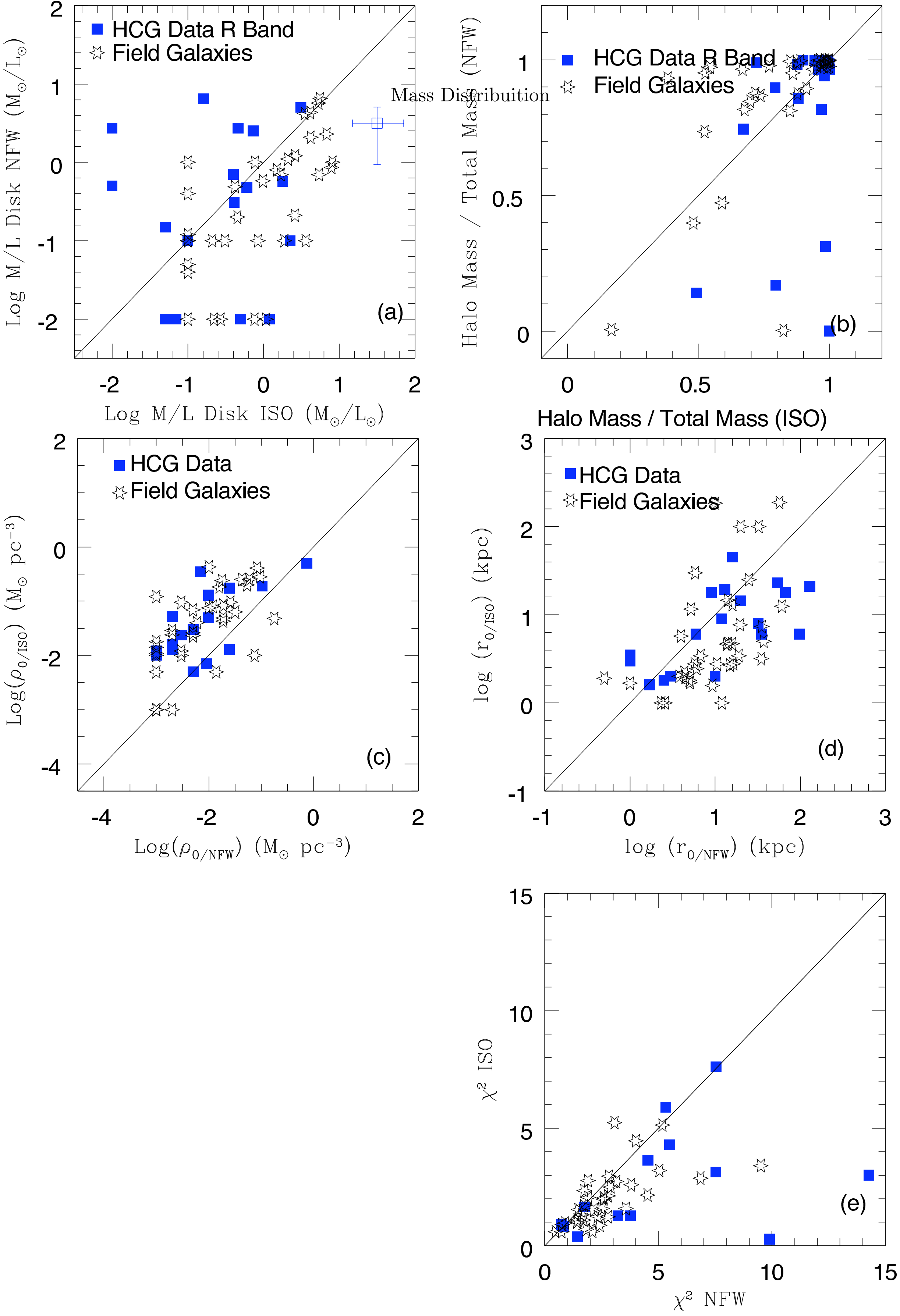

FIG. B3.— Fig. 3a: Disk M/L using ISO vs NFW for both field and HCG galaxies. Fig. 3b represents the halo mass fraction (normalised to the total mass) using ISO vs NFW for both field and HCG galaxies. Fig. 3c, d represent the comparison of the central halo density and the radius using ISO and NFW halo models. Fig 3e compares the reduced χ^2 parameter with ISO and NFW. Only 12 galaxies out 18 are shown; the others have reduced χ^2 larger than 15.